Synaptonemal Complex Proteins of Budding Yeast Define Reciprocal Roles in MutSγ-Mediated Crossover Formation

Karen Voelkel-Meiman, Shun-Yun Cheng, Savannah J. Morehouse, and Amy J. MacQueen[1]
Department of Molecular Biology and Biochemistry, Wesleyan University, Middletown, Connecticut 06459

ABSTRACT During meiosis, crossover recombination creates attachments between homologous chromosomes that are essential for a precise reduction in chromosome ploidy. Many of the events that ultimately process DNA repair intermediates into crossovers during meiosis occur within the context of homologous chromosomes that are tightly aligned via a conserved structure called the synaptonemal complex (SC), but the functional relationship between SC and crossover recombination remains obscure. There exists a widespread correlation across organisms between the presence of SC proteins and successful crossing over, indicating that the SC or its building block components are procrossover factors . For example, budding yeast mutants missing the SC transverse filament component, Zip1, and mutant cells missing the Zip4 protein, which is required for the elaboration of SC, fail to form MutSγ-mediated crossovers. Here we report the reciprocal phenotype—an increase in MutSγ-mediated crossovers during meiosis—in budding yeast mutants devoid of the SC central element components Ecm11 or Gmc2, and in mutants expressing a version of Zip1 missing most of its N terminus. This novel phenotypic class of SC-deficient mutants demonstrates unequivocally that the tripartite SC structure is dispensable for MutSγ-mediated crossover recombination in budding yeast. The excess crossovers observed in SC central element-deficient mutants are Msh4, Zip1, and Zip4 dependent, clearly indicating the existence of two classes of SC proteins—a class with procrossover function(s) that are also necessary for SC assembly and a class that is not required for crossover formation but essential for SC assembly. The latter class directly or indirectly limits MutSγ-mediated crossovers along meiotic chromosomes. Our findings illustrate how reciprocal roles in crossover recombination can be simultaneously linked to the SC structure.

KEYWORDS synapsis; crossover recombination; budding yeast

THE synaptonemal complex (SC) is correlated with successful interhomolog crossover formation during meiosis; mutants missing SC components nearly always exhibit a decrease in crossovers and (as a consequence) increased errors in chromosome segregation at meiosis I (Page and Hawley 2004). Transverse filaments establish a prominent component of the typically tripartite SC structure; transverse filaments are composed of coiled-coil proteins that form rod-like entities that orient perpendicular to the long axis of aligned chromosomes, bridging chromosome axes at a distance of ~100 nm along the entire length of the chromosome pair (Page and Hawley 2004). The largely coiled-coil Zip1 protein is a major (and perhaps the only) transverse filament protein of the budding yeast SC (Sym *et al.* 1993; Dong and Roeder 2000) (Figure 1A).

Budding yeast mutants that are missing the SC transverse filament protein Zip1 lack MutSγ-mediated crossovers (Novak *et al.* 2001; Borner *et al.* 2004; Voelkel-Meiman *et al.* 2015). Furthermore, crossover levels in double mutants missing Zip1 and any of the so-called synapsis initiation complex (SIC) proteins (Zip2, Zip3, Zip4, and Spo16), which are required for SC assembly, and in triple mutants that simultaneously lack Zip1, Zip4, and/or Msh4, indicate that SIC proteins promote the same (MutSγ-mediated) set of crossovers attributed to Zip1 function (Novak *et al.* 2001; Borner *et al.* 2004; Tsubouchi *et al.* 2006; Shinohara *et al.* 2008; Voelkel-Meiman *et al.* 2015; this work).

One exception to the strong positive correlation between SC proteins and crossover formation in budding yeast is our prior observation of elevated crossover recombination in SUMO-deficient mutants, which also exhibit diminished tripartite

doi: 10.1534/genetics.115.182923
Manuscript received September 19, 2015; accepted for publication April 17, 2016; published Early Online May 12, 2016.
Supplemental material is available online at www.genetics.org/lookup/suppl/doi:10.1534/genetics.115.182923/-/DC1.
[1]Corresponding author: 238 Hall Atwater, 52 Lawn Ave., Middletown, CT 06459. E-mail: amacqueen@wesleyan.edu

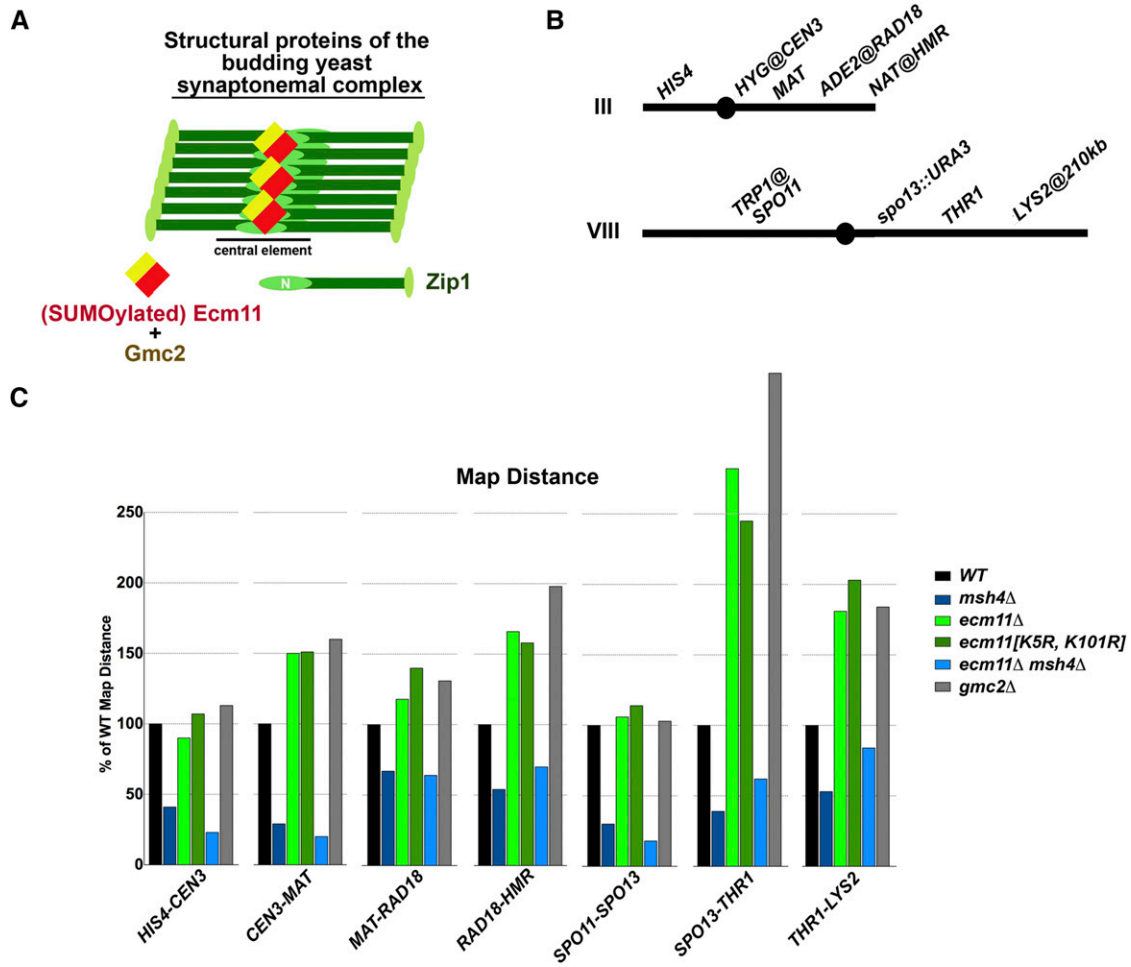

Figure 1 *ecm11* and *gmc2* mutants display excess Msh4-dependent interhomolog crossovers. (A) Proposed arrangement of known structural components of the budding yeast SC (Voelkel-Meiman *et al.* 2013): Zip1 dimer units (green) orient with N termini oriented toward the midline of the SC central region, where Ecm11 and/or SUMOylated Ecm11 (red) and Gmc2 (gold) assemble to create the SC central element substructure. (B) Markers used to define seven genetic intervals in which crossing over was assessed by tetrad analysis. (C) Percentage of wild-type map distance displayed by each strain for each interval (labeled on the *x*-axis). [See Table 1 for raw data, including significance values and strain names; Table S1 for non-Mendelian (non 2:2) segregation; and Table S3 for sporulation efficiency and viability of strains used.]

SC assembly (synapsis) (Voelkel-Meiman *et al.* 2013). Because SUMOylation is associated with a variety of molecular targets and because mutants missing the SUMOylated protein Ecm11 (a structural component of the budding yeast SC central element) were reported to exhibit reduced meiotic crossovers (Humphryes *et al.* 2013), the observation of increased crossovers in SUMO-deficient mutants was not interpreted at the time as evidence that the budding yeast SC has an antagonistic relationship with meiotic crossover formation.

The tight correlation between defects in synapsis and crossing over suggests the possibility that the SC structure itself has a functional role in meiotic crossover recombination. The maturation of recombination intermediates occurs largely within the context of assembled SC, but how the SC structure interfaces with the double strand break (DSB) repair process remains obscure. In budding yeast it is thought that at least some SC proteins facilitate early steps in interhomolog recombination that may occur prior to the elaboration of full-length SC (Storlazzi *et al.* 1996; Hunter and Kleckner 2001; Borner *et al.* 2004) leaving open the question of whether the mature SC is required at all for crossover formation. Recent genetic data from *Caenorhabditis elegans* and rice, on the other hand, have raised the paradox that while SC components are essential for meiotic crossovers, strains partially depleted for SC protein activity exhibit an increase in crossovers (Libuda *et al.* 2013; Wang *et al.* 2015). These observations indicate that SC proteins are associated with both positive and negative roles in crossing over, but it remains unknown how the pro- and anticrossover functions attributed to SC components in these organisms are related to one another at the molecular level.

Here we describe a set of SC-deficient budding yeast mutants with a novel phenotype that cleanly uncouples SC-associated crossover recombination from tripartite SC assembly. We find that structural components of the budding yeast SC can be classified into two groups based on their reciprocal affects on crossover formation: Mutants missing building blocks of the SC central

Table 1 *ecm11* and *gmc2* mutants display an excess of Msh4-dependent meiotic crossover events

Genotype (strain)	Interval (chromosome)	PD	TT	NPD	Total	cM[a]	%WT	cM by chrm	%WT by chrm	NPDobs/ NPDexp (±SE)
WT (K842)	*HIS4-CEN3* (III)	344	325	6	675	26.7 (1.4)	100	106.0 (III)	100	0.19 (0.08)
	CEN3-MAT (III)	427	250	4	681	20.1 (1.2)	100			0.25 (0.13)
	MAT-RAD18 (III)	255	405	14	674	36.3 (1.8)	100			0.22 (0.06)
	AD18-HMR (III)	395	273	6	674	22.9 (1.4)	100			0.30 (0.13)
	SPO11-SPO13 (VIII)	251	401	21	673	39.2 (2.0)	100	76.3 (VIII)	100	0.35 (0.08)
	SPO13-THR1 (VIII)	565	94	1	660	7.6 (0.8)	100			0.54 (0.54)
	THR1-LYS2 (VIII)	296	361	5	662	29.5 (1.3)	100			0.11 (0.05)
msh4Δ (K852)	*HIS4-CEN3* (III)	373	96	1	470	10.9 (1.1)	41	53.3 (III)	50	0.35 (0.35)
	CEN3-MAT (III)	424	50	1	475	5.9 (0.9)	29			1.41 (1.42)
	MAT-RAD18 (III)	275	183	7	465	24.2 (1.9)	67			0.55 (0.21)
	RAD18-HMR (III)	351	115	0	466	12.3 (1.0)	54			n.d.
	SPO11-SPO13 (VIII)	365	88	3	456	11.6 (1.4)	30	30.2 (VIII)	40	1.22 (0.71)
	SPO13-THR1 (VIII)	423	27	0	450	3.0 (0.6)	39			n.d.
	THR1-LYS2 (VIII)	320	129	2	451	15.6 (1.4)	53			0.34 (0.25)
mlh3Δ (K854)	*HIS4-CEN3* (III)	367	157	0	524	15.0 (1.0)	56	62.2 (III)	40	n.d.
	CEN3-MAT (III)	415	104	3	522	11.7 (1.3)	58			1.00 (0.58)
	MAT-RAD18 (III)	280	232	4	516	24.8 (1.5)	68			0.20 (0.10)
	RAD18-HMR (III)	408	111	0	519	10.7 (0.9)	47			n.d.
	SPO11-SPO13 (VIII)	325	185	6	516	21.4 (1.7)	55	42.2 (VIII)	55	0.53 (0.22)
	SPO13-THR1 (VIII)	475	41	0	516	4.0 (0.6)	53			n.d.
	THR1-LYS2 (VIII)	352	161	2	515	16.8 (1.3)	57			0.25 (0.18)
ecm11Δ (K857)	*HIS4-CEN3* (III)	456	371	5	832	24.1 (1.1)	90	134.9 (III)	127	0.16 (0.07)
	CEN3-MAT (III)	397	426	13	836	30.1 (1.5)	150			0.29 (0.08)
	MAT-RAD18 (III)	260	486	29	775	42.6 (2.0)	118			0.34 (0.07)
	RAD18-HMR (III)	314	453	25	792	38.1 (1.9)	166			0.41 (0.09)
	SPO11-SPO13 (VIII)	332	441	39	812	41.6 (2.2)	106	116.4 (VIII)	153	0.73 (0.13)
	SPO13-THR1 (VIII)	464	267	8	739	21.3 (1.4)	280			0.49 (0.18)
	THR1-LYS2 (VIII)	210	463	52	725	53.5 (2.7)	181			0.60 (0.11)
ecm11[K5R,K101R] (K846)	*HIS4-CEN3* (III)	299	316	6	621	28.3 (1.5)	106			0.18 (0.07)
	CEN3-MAT (III)	300	313	10	623	29.9 (1.7)	149	145.4 (III)	137	0.31 (0.10)
	MAT-RAD18 (III)	174	377	38	589	51.4 (2.9)	142			0.53 (0.11)
	RAD18-HMR (III)	254	324	17	595	35.8 (2.1)	156			0.43 (0.11)
	SPO11-SPO13 (VIII)	226	325	32	583	44.3 (2.7)	113	122.3 (VIII)	160	0.77 (0.15)
	SPO13-THR1 (VIII)	338	199	0	537	18.5 (1.0)	243			n.d.
	THR1-LYS2 (VIII)	128	364	46	538	59.5 (3.3)	202			0.65 (0.11)
gmc2Δ (K906)	*HIS4-CEN3* (III)	218	237	7	462	30.2 (1.9)	113			0.27 (0.11)
	CEN3-MAT (III)	210	244	9	463	32.2 (2.1)	160	155.3 (III)	147	0.32 (0.11)
	MAT-RAD18 (III)	136	278	23	437	47.6 (3.1)	131			0.45 (0.11)
	RAD18-HMR (III)	117	310	15	442	45.3 (2.5)	198			0.43 (0.04)
	SPO11-SPO13 (VIII)	183	249	19	451	40.2 (2.8)	103	120.9 (VIII)	158	0.61 (0.15)
	SPO13-THR1 (VIII)	231	178	7	416	26.4 (2.1)	347			0.50 (0.19)
	THR1-LYS2 (VIII)	103	277	28	408	54.3 (3.5)	184			0.55 (0.09)
ecm11Δ msh4Δ (K882)	*HIS4-CEN3* (III)	358	51	0	409	6.2 (0.8)	23	49.6 (III)	47	n.d.
	CEN3-MAT (III)	382	28	1	411	4.1 (1.0)	20			4.00 (4.02)
	MAT-RAD18 (III)	237	153	5	395	23.2 (2.0)	64			0.48 (0.22)
	RAD18-HMR (III)	292	105	4	401	16.1 (1.8)	70			0.95 (0.48)
	SPO11-SPO13 (VIII)	338	56	0	394	7.1 (0.9)	18	36.5 (VIII)	48	n.d.
	SPO13-THR1 (VIII)	340	35	0	375	4.7 (0.8)	62			n.d.
	THR1-LYS2 (VIII)	244	118	11	373	24.7 (2.8)	84			1.82 (0.58)
ecm11Δ mlh3Δ (K888)	*HIS4-CEN3* (III)	343	109	4	456	14.6 (1.6)	55	79.5 (III)	75	1.02 (0.52)
	CEN3-MAT (III)	330	108	2	440	13.6 (1.4)	68			0.50 (0.36)
	MAT-RAD18 (III)	207	166	14	387	32.2 (2.9)	89			1.06 (0.30)
	RAD18-HMR (III)	268	129	4	401	19.1 (1.8)	83			0.59 (0.30)
	SPO11-SPO13 (VIII)	272	148	8	428	22.9 (2.2)	58	68.9 (VIII)	90	0.93 (0.34)
	SPO13-THR1 (VIII)	324	56	1	381	8.1 (1.2)	107			0.87 (0.88)
	THR1-LYS2 (VIII)	168	179	16	363	37.9 (3.2)	128			0.89 (0.24)

Map distances and interference values were calculated using tetrad analysis and coefficient of coincidence measurements as described previously (Voelkel-Meiman *et al.* 2015). Four-spore viable tetrads with no more than two gene conversion (non-2:2) events were included in calculations, although cases where adjacent loci display non-2:2 segregation were considered a single (co-conversion) event. See Table S1 for gene conversion frequencies. Table indicates the number of tetratype (TT), parental ditype (PD) and nonparental ditype (NPD) tetrads scored, map distances (in centimorgans; cM) and their corresponding percentages of the wild-type values for individual intervals, and the map distances and the corresponding percentage of wild type for the entire chromosome (chrm) by summing the intervals on III or VIII. The table also indicates the ratio of observed (obs) to expected (exp) NPD tetrads. The number of chromatids III participating in crossover recombination indicates a general increase in interhomolog events in *ecm11* mutants relative to wild type: In wild-type four-spore viable tetrads ($n = 512$), all of the crossover events on chromosome III in a given tetrad involved two chromatids 45% of the time, three chromatids 26% of the time, and four chromatids 27% of the time. In four-spore viable tetrads from *ecm11* mutants ($n = 878$), all of the crossover events on chromosome III in a given tetrad involved two chromatids only 27% of the time, three chromatids 33% of the time, and four chromatids 37% of the time. For the intervals marked with n.d., interference measurements are not obtainable using the coefficient of coincidence method due to an absence of NPD tetrads.
[a] ±SE

element, Ecm11 or Gmc2 (Humphryes *et al.* 2013; Voelkel-Meiman *et al.* 2013), and strains expressing a version of Zip1 that is missing most of its N terminus (the *zip1-N1* mutant allele) (Tung and Roeder 1998), do not exhibit the deficiency in crossing-over characteristic of previously described synapsis-deficient mutants. Instead, *ecm11*, *gmc2*, and *zip1-N1* mutants display an increase in MutSγ-mediated crossing over. Our findings demonstrate that the tripartite SC structure is dispensable for "pro" crossover recombination functions in budding yeast, and these data furthermore suggest that elaborated SC structure directly or indirectly limits the formation of MutSγ-mediated interhomolog crossovers during meiosis.

Materials and Methods

Strains and genetic analysis

Yeast strains used in this study are isogenic to BR1919-8B (Rockmill and Roeder 1998; Supplemental Material, Table S4) and were generated using conventional crossing and genetic manipulation procedures. Two distinct sets of markers were used for tetrad analysis experiments shown in Table 1 and Table 2. Both strains carry an *hphMX4* cassette inserted near the chromosome III centromere, *ADE2* inserted upstream of the *RAD18* locus, a *natMX4* cassette inserted near the *HMR* locus, *TRP1MX4* inserted 62 bp downstream of the *SPO11* locus (Kee and Keeney 2002), and *URA3* replacing *SPO13*. In strains linked to Table 1, *LYS2* was inserted on chromosome VIII at coordinate 210,400 bp. In strains linked to Table 2, *LEU2* and *THR1* were inserted on chromosome XI at chromosomal coordinates 152,000 and 193,424 bp, respectively. Tetrad analysis, crossover interference analyses, and prototroph experiments were carried out on solid media, as previously described (Voelkel-Meiman *et al.* 2015). All statistical analyses were performed using GraphPad InStat software.

Physical assays, pulsed field gel electrophoresis, and Southern blotting

Agarose plugs were prepared from meiotic cultures at 0, 40, and 70 hr of sporulation and subjected to pulsed-field gel analysis. For Southern blotting, a 1-kb probe from the *THR4* region of chromosome III was prepared using a DIG High Prime DNA Labeling and Detection Kit (Roche). A Syngene "G:Box" was used to detect chemiluminescence and the Syngene Gene Tools program was used to analyze the data. A value for percentage of recombination was calculated by summing twice the intensity of the trimer band (a double crossover product) plus the dimer band (product of a single crossover) over the total intensity of the three bands (trimer, dimer, and monomer). Note that circular chromosome III chromatids do not enter the gel, and thus are not included in the calculation to estimate recombination. The average of two experiments is presented.

Western blot

Protein pellets were isolated from 5 ml of sporulating cell culture by trichloroacetic acid precipitation as in Hooker and Roeder (2006). The final protein pellet was suspended in 2× Laemmli sample buffer supplemented with 30 mM DTT at a concentration of ~10 μg/μl. Protein samples were heated for 10 min at 65°, centrifuged at top speed, and ~100 μg was loaded onto an 8% polyacrylamide/SDS gel. PVDF membranes were prepared according to the manufacturer's (Bio-Rad) recommendation, equilibrating with Towbin buffer for 15 min after methanol wetting. Transfer of proteins to PVDF membranes was done following the Bio-Rad Protein Blotting Guide for tank blotting using Towbin buffer; stir bar and ice pack were used and transfer was done at 60 V for 1 hr. Ponceau S was used to detect relative protein levels on the PVDF membrane after transfer. Mouse anti-MYC (9E10; Invitrogen) was used at 1:2500. Incubations with primary antibody were performed overnight at 4°. HRP-conjugated AffiniPure goat anti-mouse antibody (Jackson ImmunoResearch) was used at 1:5000 in TBS-T for 1 hr at RT. Amersham ECL Prime Western Blotting Detection Reagent was used to visualize antibodies on the membranes; a Syngene G:Box and the Syngene GeneTools program was used to detect and analyze the data.

Cytological analysis and imaging

Meiotic chromosome spreads, staining, and imaging were carried out as previously described (Rockmill 2009) with the following modifications: 80 μl 1× 2-(N-morpholino)-ethanesulfonic acid and 200 μl 4% paraformaldehyde fix were added to spheroplasted, washed cells, then 80 μl of resuspended cell solution was put directly onto a frosted slide, and cells were distributed over the entire slide using the edge of a coverslip with moderate pressure. The slide was allowed to air dry until less than half of the liquid remained and then washed in 0.4% Photo-Flo as described. The following primary antibodies were used: mouse anti c-MYC (1:200) (9E10; Invitrogen), affinity purified rabbit anti-Zip1 (1:100) [raised at YenZym Antibodies against a C-terminal fragment of Zip1 as described in Sym *et al.* (1993)], rat anti-α-tubulin antibody (Santa Cruz Biotechnology). Secondary antibodies were obtained from Jackson ImmunoResearch and used at a 1:200 dilution. Imaging was carried out using the Deltavision RT Imaging System (Applied Precision) adapted to an Olympus (IX71) microscope.

Cells were prepared for multinucleate analysis (Figure S2B) by first transferring them from solid sporulation media into cold 50% ethanol, and storing fixed cells at −20° until all time points were collected. Next, 1 μl of fixed cells were transferred to a single well of a multiwell slide and allowed to dry. Vectashield mounting medium (Vector Laboratories) containing 1 μg/ml DAPI was placed on top of the dried cells and a cover slip was added.

Data availability

The authors state that all data necessary for confirming the conclusions presented in the article are represented fully within the article.

Table 2 *zip1-N1* expressing meiotic cells display the same excess of Msh4-dependent interhomolog crossovers observed in *ecm11* mutants

Genotype (strain)	Interval (chromosome)	PD	TT	NPD	Total	cM (±SE)	%WT	cM by chrm	%WT by chrm	NPDobs/NPDexp (±SE)
WT (YT131)	*HIS4-CEN3* (III)	257	231	8	496	28.1 (1.9)	100			0.38 (0.14)
	CEN3-MAT (III)	340	155	3	498	17.4 (1.4)	100	107.4 (III)	100	0.39 (0.22)
	MAT-RAD18 (III)	187	288	16	491	39.1 (2.4)	100			0.38 (0.11)
	RAD18-HMR (III)	295	196	5	496	22.8 (1.7)	100			0.37 (0.17)
	SPO11-SPO13 (VIII)	219	260	6	485	30.5 (1.7)	100			0.20 (0.08)
	iTHR1-iLEU2 (XI)	403	90	0	493	9.1 (0.9)	100			n.d.
msh4Δ (AM3313)	*HIS4-CEN3* (III)	521	90	3	614	8.8 (1.1)	31			1.64 (0.95)
	CEN3-MAT (III)	526	90	3	619	8.7 (1.1)	50	59.2 (III)	55	1.65 (0.96)
	MAT-RAD18 (III)	362	230	12	604	25 (1.9)	64			0.79 (0.24)
	RAD18-HMR (III)	441	162	7	610	16.7 (1.5)	73			1.1 (0.41)
	SPO11-SPO13 (VIII)	465	129	2	596	11.8 (1.1)	39			0.49 (0.35)
	iTHR1-iLEU2 (XI)	587	33	0	620	2.7 (0.5)	30			n.d.
ecm11Δ (AM3378)	*HIS4-CEN3* (III)	158	217	4	379	31.8 (1.9)	113			0.14 (0.07)
	CEN3-MAT (III)	159	215	4	378	31.6 (1.9)	182	151.3 (III)	141	0.14 (0.17)
	MAT-RAD18 (III)	101	232	21	354	50.6 (3.5)	129			0.43 (0.12)
	RAD18-HMR (III)	128	229	7	364	37.2 (2.3)	163			0.17 (0.07)
	SPO11-SPO13 (VIII)	115	224	20	362	47.9 (3.5)	157			0.50 (0.13)
zip1-N1 (SYC123)	*HIS4-CEN3* (III)	265	303	12	580	32.2 (1.9)	115			0.35 (0.11)
	CEN3-MAT (III)	209	375	17	601	39.7 (2.1)	228	147.9 (III)	138	0.26 (0.07)
	MAT-RAD18 (III)	215	355	17	587	38.9 (2.1)	100			0.30 (0.08)
	RAD18-HMR (III)	242	329	18	589	37.1 (2.2)	163			0.42 (0.11)
	SPO11-SPO13 (VIII)	144	391	40	575	54.9 (2.9)	181			0.56 (0.08)
	iTHR1-iLEU2 (XI)	417	164	5	586	16.6 (1.4)	184			0.70 (0.32)
zip1-N1 ecm11Δ (SYC142)	*HIS4-CEN3* (III)	290	459	12	761	34.9 (1.5)	125			0.17 (0.05)
	CEN3-MAT (III)	262	498	18	778	39.0 (1.7)	224	147.1 (III)	137	0.19 (0.05)
	MAT-RAD18 (III)	302	428	21	751	36.9 (1.9)	94			0.36 (0.09)
	RAD18-HMR (III)	307	427	20	754	36.3 (1.8)	159			0.35 (0.08)
	SPO11-SPO13 (VIII)	198	501	50	749	53.5 (2.5)	175			0.43 (0.07)
	iTHR1-iLEU2 (XI)	432	313	8	753	24.0 (1.4)	264			0.34 (0.12)
zip1-N1 msh4Δ (SYC151)	*HIS4-CEN3* (III)	481	116	2	599	10.7 (1.1)	38			0.62 (0.44)
	CEN3-MAT (III)	496	109	2	607	10.0 (1.0)	57	147.1 (III)	54	0.73 (0.52)
	MAT-RAD18 (III)	407	185	6	598	18.5 (1.5)	47			0.65 (0.27)
	RAD18-HMR (III)	397	199	4	600	18.6 (1.3)	82			0.37 (0.19)
	SPO11-SPO13 (VIII)	437	138	2	577	13.0 (1.1)	43			0.40 (0.29)
	iTHR1-iLEU2 (XI)	503	73	0	576	6.3 (0.7)	69			n.d.
zip1-N1 mlh3Δ (SYC133)	*HIS4-CEN3* (III)	312	157	6	475	20.3 (1.8)	72			0.70 (0.29)
	CEN3-MAT (III)	274	205	12	491	28.2 (2.2)	162	110.5 (III)	103	0.77 (0.23)
	MAT-RAD18 (III)	246	226	13	485	31.3 (2.3)	80			0.63 (0.19)
	RAD18-HMR (III)	253	221	13	487	30.7 (2.3)	135			0.68 (0.20)
	SPO11-SPO13 (VIII)	215	236	20	471	37.8 (2.8)	124			0.82 (0.20)
	iTHR1-iLEU2 (XI)	371	103	2	476	12.1 (1.3)	133			0.61 (0.43)

Map distances and interference values were calculated using tetrad analysis as described previously (Voelkel-Meiman *et al.* 2015). Four-spore viable tetrads with no more than two gene conversion (non-2:2) events were included in calculations, although cases where adjacent loci display non-2:2 segregation were considered a single (co-conversion) event. See Table S1 for gene conversion frequencies. Table indicates the number of tetratype (TT), parental ditype (PD) and nonparental ditype (NPD) tetrads scored, map distances (in centimorgans; cM) and their corresponding percentages of wild-type values for individual intervals, and map distances and corresponding percentage of wild type for the entire chromosome (chrm) III (by summing the intervals on III). The table also indicates the ratio of observed (obs) to expected (exp) NPD tetrads. For the intervals marked with n.d., interference measurements are not obtainable due to an absence of NPD tetrads. Data for wild-type and *msh4* strains were previously reported (Voelkel-Meiman *et al.* 2015).

Results and Discussion

Excess interhomolog crossovers form in ecm11 and gmc2 mutants

In budding yeast and in many other organisms, a "central element" substructure lies at the midline of the SC (Hamer *et al.* 2006; Voelkel-Meiman *et al.* 2013). SUMOylated and unSUMOylated Ecm11, and (by extension) the Ecm11-interacting protein Gmc2, are components of the central element substructure, which assembles close to Zip1's N termini within the mature budding yeast SC (Humphryes *et al.* 2013; Voelkel-Meiman *et al.* 2013). In stark contrast to the reduced meiotic recombination frequencies observed in strains missing any of several other proteins required for SC assembly in budding yeast, such as *zip1*, *zip2*, *zip4*, and *spo16* mutants (Sym and Roeder 1994; Chua and Roeder 1998; Borner *et al.* 2004; Tsubouchi *et al.* 2006; Shinohara *et al.* 2008; Voelkel-Meiman *et al.* 2015), we discovered that meiotic interhomolog

crossovers are elevated in synapsis defective, *ecm11* and *gmc2* mutants (Figure 1, B–C; Table 1). Tetrad analysis was used to measure crossover frequency in seven intervals on chromosomes III and VIII. In six of seven intervals, crossovers in *ecm11* (null), *ecm11[K5R, K101R]* (non-SUMOylatable), or *gmc2* mutants are elevated to 113–280% of the wild-type level (Figure 1C, Table 1). Thus, unlike the transverse filament component Zip1 and other prosynapsis factors in budding yeast, Ecm11 and Gmc2 are structural components of budding yeast SC that are dispensable, *per se*, for meiotic crossing over.

We also measured non-Mendelian segregation, a reflection of gene conversion resulting from interhomolog recombination (both crossover and noncrossover) events, for every marker included in our crossover recombination analysis. Consistent with our observation of an elevation in the number of interhomolog crossovers, a four- to sevenfold increase in overall gene conversion levels was observed in *ecm11*, *ecm11[K5R, K101R]*, and *gmc2* mutants relative to wild type (Table S1). These data indicate that both crossover and noncrossover interhomolog recombination events are elevated when Ecm11 or Gmc2 is absent.

The excess crossovers in ecm11 mutants are dependent on MutSγ

Mutants missing the Msh4 component of MutSγ exhibit 29–73% of the wild-type crossover level, depending on the interval examined (Figure 1C, Figure 2, Figure 3C, Table 1, Table 2). The diminished crossover phenotype observed in *msh4* mutant cells is epistatic to the excess crossover phenotype of *ecm11* strains: The *ecm11 msh4* double mutant exhibits crossover levels that are similar to the low levels of the *msh4* single mutant (Figure 1C, Table 1). Thus, unlike the excess crossovers observed in strains deficient for Sgs1 helicase activity during meiosis (Jessop *et al.* 2006), the additional crossovers in *ecm11* mutants are MutSγ mediated.

Under normal circumstances, the resolution of most crossover-designated recombination intermediates in budding yeast is dependent on MutLγ (Kolas and Cohen 2004; Zakharyevich *et al.* 2012). Removal of the MutLγ component, Mlh3 from *ecm11* mutant strains results in a reduced number of interhomolog crossovers, although to a lesser extent than *ecm11 msh4* double mutants: the interhomolog crossover frequency displayed by *ecm11 mlh3* double mutants appeared midway between the low crossover frequency of *msh4* and the high crossover frequency of *ecm11* mutant strains (Table 1). This observation is consistent with the proposal that MutLγ is not *per se* essential for the resolution of MutSγ intermediates but if present, channels those intermediates in a biased manner toward a crossover outcome (De Muyt *et al.* 2012; Zakharyevich *et al.* 2012). Accordingly, in the absence of MutLγ activity, MutSγ crossover-designated intermediates are presumably resolved in an unbiased manner by structure-selective nucleases such that they give rise to both crossovers and noncrossovers with equal frequency.

Surprisingly, removal of Mlh3 from *ecm11* mutants results in double the frequency of non-Mendelian segregation relative to the *ecm11* single mutant (Table S1). Given the fact that the frequency of gene conversion in the *mlh3* single mutant resembles wild-type meiotic cells, the elevated frequency in the *ecm11 mlh3* double mutant suggests that Mlh3 acts synergistically with Ecm11 in an activity that ultimately limits interhomolog recombination.

The MutSγ-mediated crossovers in ecm11 mutants rely on Zip1 and Zip4 proteins

Using a physical assay for recombination, we observed that the excess crossovers that occur when SC central element protein Ecm11 is absent relies on the SC transverse filament protein, Zip1, as well as on the synapsis initiation complex protein, Zip4. The "circle-linear" assay estimates crossover frequency based on the relative abundance of crossover chromatid products resulting from recombination between circular and linear chromosomes III (Game *et al.* 1989; Voelkel-Meiman *et al.* 2015) (See Figure 2 legend). A limitation of the assay, which is relevant to this study, is that it underestimates crossover frequency (since chromosomes with more than two crossovers are not detectable), and thus likely will not report increases above the wild-type crossover frequency. However, the circle-linear assay is a powerful tool for detecting a reduction in crossing over, particularly for mutants such as *zip1* and *zip4* where diminished spore production in our strain background precludes tetrad analysis. Using the circle-linear assay, a prior study reported a delay and overall reduction in the accumulation of crossovers in *ecm11* and *gmc2* mutants at time points through 48 hr of sporulation (Humphryes *et al.* 2013). In our analysis of *ecm11*, *ecm11[K5R, K101R]*, and *gmc2* mutants using the circle-linear assay, a mild reduction in the accumulation of resolved crossover recombination intermediates was observed at 40 hr of sporulation, but an approximately wild-type crossover frequency was observed for these mutants at 70 hr (Figure 2). The wild-type crossover frequency observed in *ecm11*, *ecm11[K5R, K101R]*, and *gmc2* mutants at 70 hr is in sharp contrast to the diminished frequency (~30%) measured in the SC-deficient *zip1* and *zip4* mutants at this time point (Figure 2). Our analysis using this assay moreover revealed that crossovers diminish to *zip1*, *zip4*, *msh4*, or *msh5* single mutant levels when Zip1, Zip4, Msh4, and Msh5, respectively, are removed from *ecm11* mutant strains (Figure 2). Thus the extra crossovers formed in *ecm11* mutants (observed by genetic analysis) rely not only on the Msh4–Msh5 complex, but on Zip1 and Zip4 proteins as well.

Altogether, our data reveal that two classes of SC structural proteins exist in budding yeast. The SC transverse filament component Zip1 is essential for building tripartite SC and for MutSγ-mediated crossover formation, while the central element components Ecm11 and Gmc2 are essential for tripartite SC assembly but dispensable for Zip1/Zip4/MutSγ-mediated crossing over. While dispensable for crossing over *per se*, the delayed accumulation of crossovers observed in

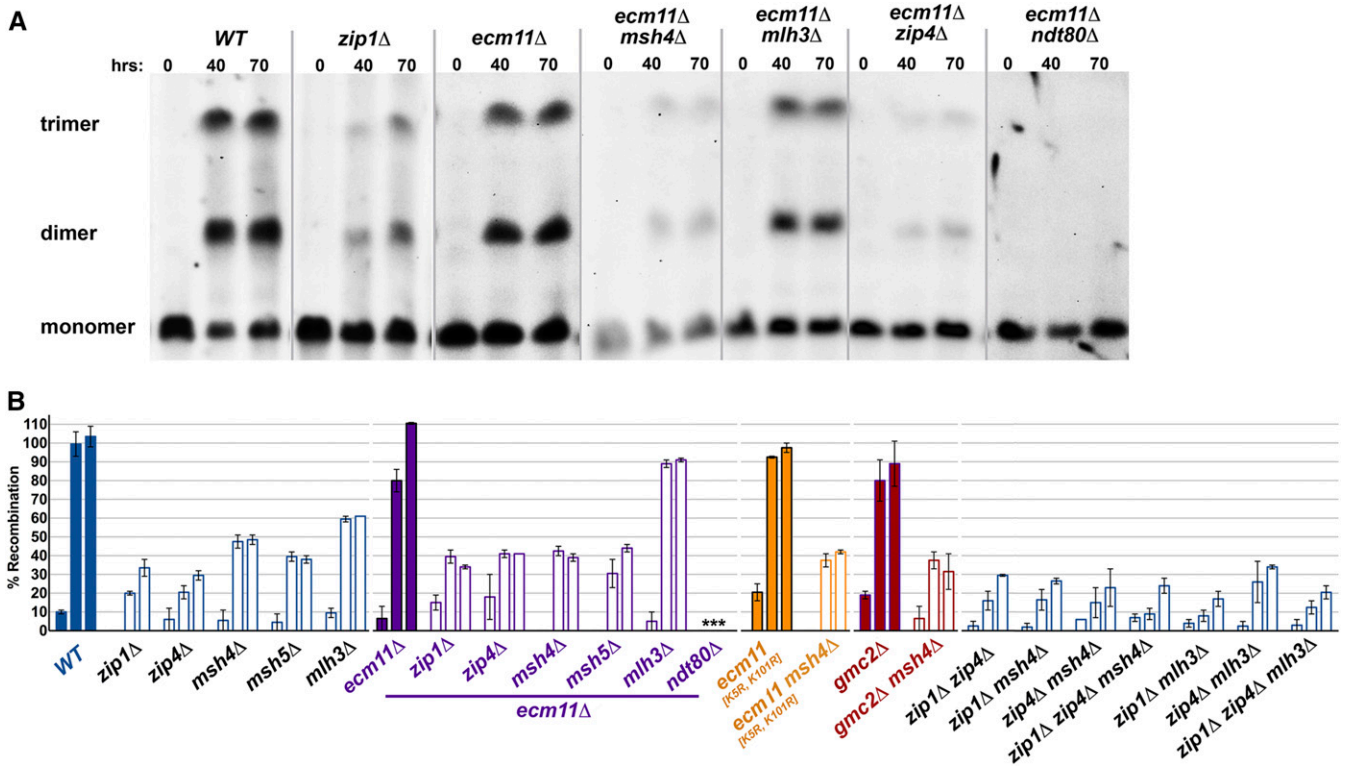

Figure 2 *ecm11* and *gmc2* mutants exhibit robust Zip1-, Zip4-, and Msh4-mediated crossing over. A physical assay for crossing over across the entire chromosome III; Southern blotting is used to measure the relative amounts of three forms of chromosome III during a meiotic time course. Aliquots of sporulating cells were taken at 0, 40, and 70 hr after placement in sporulation medium (Game 1992; Voelkel-Meiman *et al.* 2015). (A) Representative blots show bands that correspond to different sized versions of linear chromosome III present in meiotic extracts from strains indicated above the blot. Circular chromosomes III present in these strains do not enter the gel. The lowest molecular weight band represents linear (monomer) III, while the middle and upper bands represent crossover products between linear and circular III; the product of a single crossover event runs at the size of the middle band (dimer), while a double crossover event involving three sister chromatids (of which two are circular) produces the upper band, a trimer chromatid III. (B) Graph plots three bars (0, 40, or 70 hr) for each strain (indicated on the *x*-axis), of which each corresponds to a percentage of recombination estimate (calculated by summing twice the intensity of the trimer band with the dimer band and dividing the sum by the total intensity of the three bands). See Table S4 for strain names; the data for several controls have been published previously (Voelkel-Meiman *et al.* 2015).

ecm11 and *gmc2* mutants (Humphryes *et al.* 2013) does suggest that Ecm11 and Gmc2 indirectly or directly influence the rate that crossovers form, likely through promoting the timely resolution of crossover-designated intermediates at the end of prophase (see below).

A zip1 allele missing N-terminal residues exhibits elevated MutSγ-dependent crossing over

We next identified a *zip1* nonnull allele that separates Zip1's role in SC formation from its role in mediating MutSγ-dependent recombination. The *zip1-N1* allele encodes a protein missing residues 21-163, corresponding to the majority of N terminal residues upstream of Zip1's extended central coiled-coil region (Tung and Roeder 1998; Figure 3A). Prior analysis of crossing over within two adjacent intervals on chromosome III in *zip1-N1* meiotic cells of an SK1 strain background revealed an increase in crossover recombination in the *CEN3-MAT* interval, to 114% of the wild-type level, and a ~30% decrease in crossing over in the *HIS4-CEN3* interval (Tung and Roeder 1998). We performed tetrad analysis on *zip1-N1* mutants of a BR1919-derived background (Rockmill and Roeder 1998) and found elevated crossing over, corresponding to 115–228% of wild-type levels, in five of six genetic intervals representing regions of chromosomes III, VIII, and XI (Figure 3C, Table 2). Only one interval in *zip1-N1* mutants showed a wild-type crossover frequency. Our findings demonstrate that at least in the BR1919 background, crossover recombination is elevated above the wild-type level in *zip1-N1* mutant cells.

We next explored how the excess crossovers identified in *zip1-N1* mutants are related to the excess crossovers we observed in *ecm11* mutants. Crossover levels in *zip1-N1 ecm11* double mutants were not dramatically different from either single mutant, indicating that Ecm11 and Zip1-N1 proteins interface with the same crossover control pathway. Accordingly, crossover levels are reduced in *zip1-N1* mutants when either *MSH4* or *MLH3* activities are absent (Figure 3C, Table 2).

zip1-N1 mutants display an increase in non-Mendelian segregation at markers on both chromosomes III and VIII relative to wild type (Table S1). However, overall gene conversion levels (a measure of total interhomolog events) in *zip1-N1* strains are approximately half the levels observed

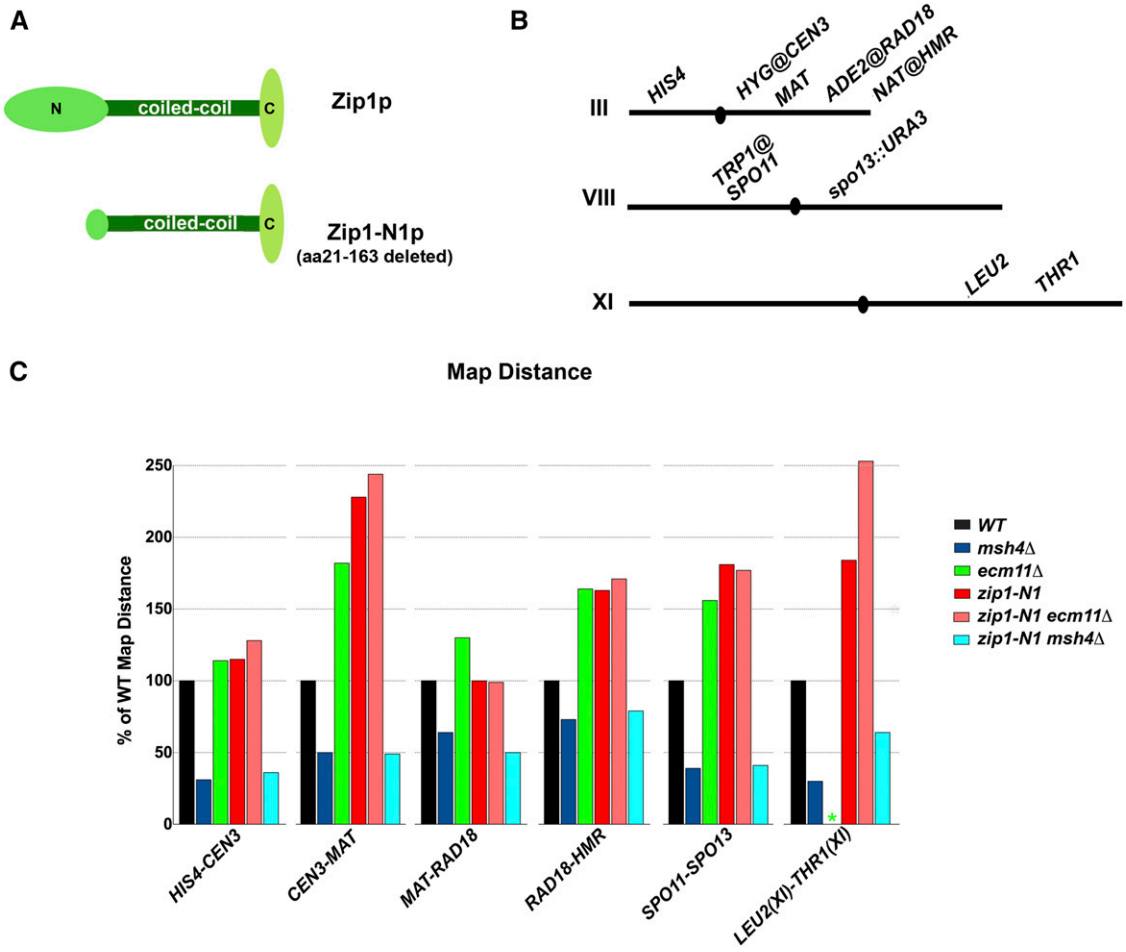

Figure 3 *zip1-N1*-expressing meiotic cells display the same excess of Msh4-dependent interhomolog crossovers observed in *ecm11* mutants. (A) The protein encoded by *zip1-N1* (Tung and Roeder 1998) is depicted below wild-type Zip1. (B) Markers used to define six genetic intervals in which crossing over was assessed (genetic markers differ from the experiment presented in Figure 1). (C) Percentage of wild-type map distance displayed by each strain for each interval (labeled on the *x*-axis). [See Table 2 for raw data (including significance values) and strain names; Table S1 for non-Mendelian segregation; and Table S3 for sporulation efficiency and viability of strains used]. Data for wild type and *msh4* were previously reported (Voelkel-Meiman *et al.* 2015). *The *LEU2–THR1* interval is absent from the *ecm11* strain.

in *ecm11*, *ecm11[K5R, K101R]*, and *gmc2* mutants, despite the fact that interhomolog crossover recombination is increased to similar levels in these mutants (Table 2). Based on these data, we surmise that a substantial fraction of the excess interhomolog recombination events observed in *ecm11* and *gmc2* mutants are associated with a noncrossover outcome. Interestingly, *zip1-N1* is epistatic to *ecm11* with respect to its gene conversion phenotype, revealing a potential role for Zip1 in influencing the number of interhomolog noncrossover recombination events that occur when Ecm11 is absent.

The zip1-N1 allele encodes a separation-of-function protein that fails to assemble tripartite SC

Although the precise molecular relationship between budding yeast transverse filaments and central element proteins remains unknown, the Ecm11 and Gmc2 central element proteins localize near Zip1's N termini within the tripartite SC (Voelkel-Meiman *et al.* 2013). We therefore reasoned that the shared phenotype of *ecm11*, *gmc2*, and *zip1-N1* mutants may be caused by a failure to assemble the central element substructure of the tripartite SC. Based on the electron microscopy done in an earlier study (Tung and Roeder 1998), at least some pachytene-stage chromosome axes in *zip1-N1* meiotic nuclei appeared intimately aligned along their entire lengths, suggesting that normal SC might assemble using Zip1-N1 protein as a building block. Importantly, however, this earlier study also found that ~97% of meiotic nuclei at 13, 15, and 17 hr of sporulation exhibited either no Zip1-N1 accumulation, or a "dotty" Zip1-N1 distribution pattern on chromosomes (Tung and Roeder 1998). Based on our observation of elevated crossing over in *zip1-N1* strains, we hypothesized that the intimate alignment between meiotic chromosome axes in *zip1-N1* mutants reflects pseudosynapsis arising as a consequence of numerous interhomolog recombination intermediates that promote local points of association along the length of chromosomes (Jessop *et al.* 2006), and not from an assembled tripartite SC structure.

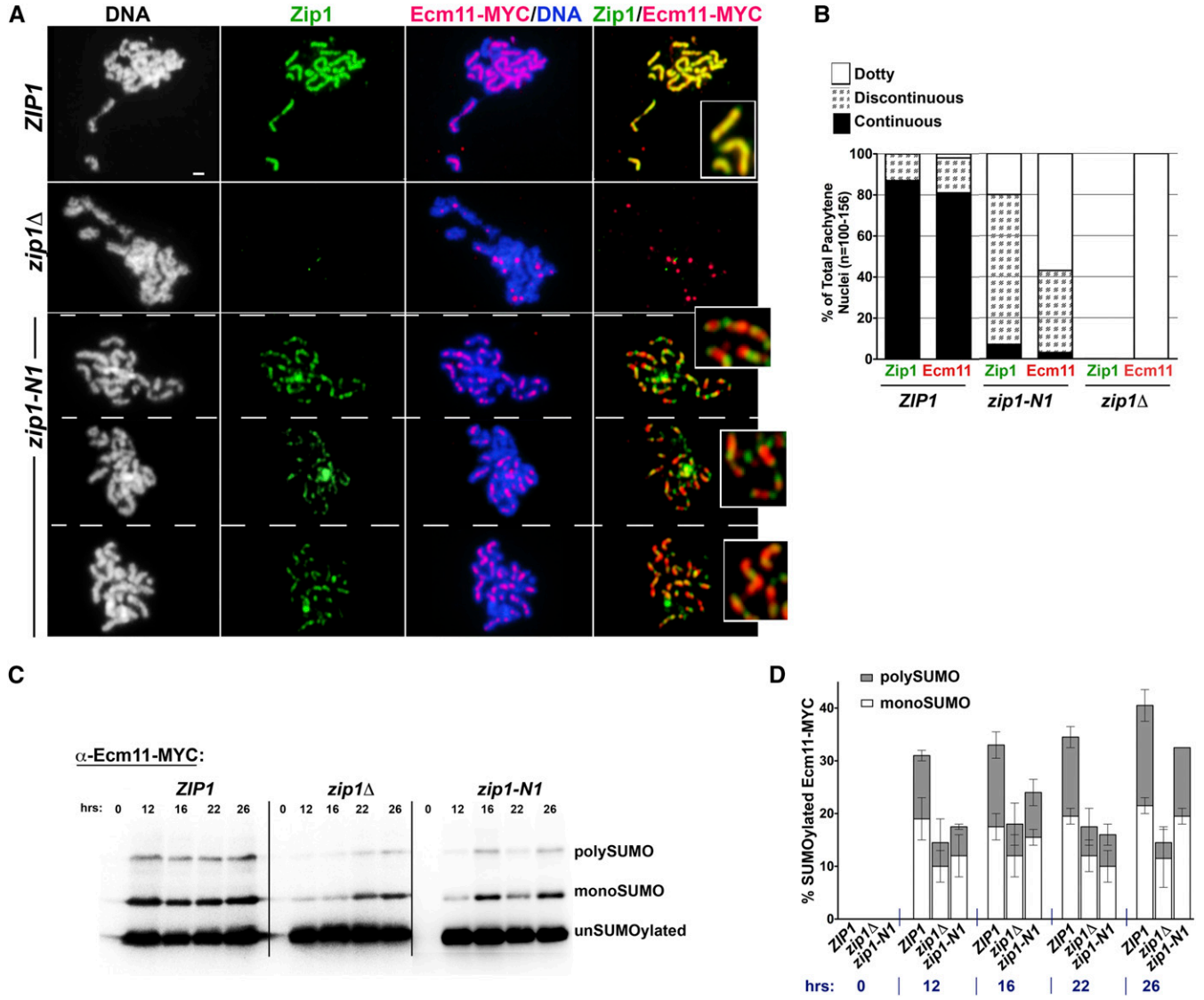

Figure 4 Ecm11 fails to assemble coincidently with Zip1-N1 on meiotic chromosomes and Ecm11 SUMOylation is altered in *zip1-N1* meiotic cells. (A) Images display surface-spread meiotic prophase-stage chromosomes from strains carrying one copy of *ECM11-MYC* and homozygous for *ZIP1* (top row), *zip1* (second row), or *zip1-N1* (bottom three rows). Strains are homozygous for an *ndt80* null allele, and thus will not progress beyond the pachytene stage of meiotic prophase (Xu *et al.* 1995). Zip1 (green) and Ecm11-MYC (red) assemble extensive, coincident linear structures on wild-type meiotic chromosomes (labeled with DAPI; white or blue), but assemble only short stretches and often do not overlap on meiotic chromosomes from *zip1-N1* strains. Insets in final column show a zoomed region from the corresponding image. Bar, 1 μm. (B) Stacked columns indicate the percentage of nuclei from each strain exhibiting absent or exclusively foci of Zip1 or Ecm11 (None or Dotty; open), a mixture of Dotty and short linear Zip1 or Ecm11 structures (Discontinuous; boxed), or long, linear Zip1 or Ecm11 structures (Continuous; solid) on late meiotic prophase chromosomes (n = 100–156). (C) Western blot shows unSUMOylated, monoSUMOylated, and polySUMOylated forms of Ecm11-MYC from *ZIP1*, *zip1*, or *zip1-N1* meiotic extracts, prepared as previously described (Humphryes *et al.* 2013; Voelkel-Meiman *et al.* 2013). (D) Percentage of monoSUMOylated (open bar) or polySUMOylated (shaded bar) forms of Ecm11-MYC measured at multiple time points for each strain. Error bars represent the range of values from two experiments (the absence of a bar associated with *zip1-N1*'s polySUMOylated Ecm11-MYC at 26 hr is due to the fact that the same value was obtained in both experiments).

Indeed, when we analyzed the distribution of Ecm11-MYC and Zip1 proteins on surface-spread meiotic chromosomes, we discovered that normal SC fails to assemble in *zip1-N1* mutants (Figure 4, A and B). Wild-type meiotic nuclei at the pachytene stage of prophase exhibit completely coincident Zip1 and Ecm11 assembled along the full length of aligned homolog pairs. The coincident labeling of Zip1 and Ecm11 reflects the interdependent arrangement of these central element and transverse filament proteins within the higher-order architecture of the wild-type SC (Figure 4A and Voelkel-Meiman *et al.* 2013). In *zip1-N1* mutants however, Zip1-N1 and Ecm11 proteins each assemble foci and very short linear stretches, and Zip1-N1 structures do not robustly coincide with Ecm11 assemblies on chromosomes (zoomed insets, Figure 4A). Consistent with an SC assembly defect, Ecm11 SUMOylation, which is required for SC assembly

and normally relies to a large extent on Zip1 (Humphryes *et al.* 2013), is diminished and severely delayed in *zip1-N1* mutants (Figure 4, C and D).

Taken together, the shared phenotype of the *ecm11*, *gmc2*, and *zip1-N1* mutants suggests the possibility that assembly of the SC central element limits MutSγ interhomolog crossover formation. A direct or an indirect mechanism could account for how assembled SC limits interhomolog crossovers, as discussed below.

Crossover interference is weakened slightly in ecm11, gmc2, and zip1-N1 mutants

MutSγ-mediated crossovers display positive interference, in that detectable double crossover events in a given chromosomal region occur less frequently than expected based on a random distribution (Novak *et al.* 2001; Nishant *et al.* 2010). While SC components are required for the successful generation of interfering (MutSγ) crossovers, other studies have suggested that SC is dispensable for crossover interference (Fung *et al.* 2004; Zhang *et al.* 2014a,b). We used coefficient of coincidence (Papazian 1952) and interference ratio (Malkova *et al.* 2004) methods to ask whether the SC-independent, MutSγ-mediated crossovers in *ecm11* and *gmc2* mutants exhibit interference. Wild-type strains displayed robust crossover interference in all intervals using either method (Table 1, Figure S1, Table S2), whereas each method indicated weakened crossover interference in *msh4*, *ecm11*, *ecm11[K5R, K101R]*, and *gmc2* mutants, although we note that most of the interference measurements for *msh4* strains are not statistically significant due to an insufficient number of crossover events. In *ecm11*, *ecm11[K5R, K101R]*, *gmc2*, and *zip1-N1* mutants (where Msh4-mediated crossovers are in excess), the ratio of $_{\text{observed/expected}}$ non-parental ditype (NPD) tetrads appeared as robust as wild type in some intervals but weaker in others, particularly in the *SPO11–SPO13* interval on chromosome VIII.

Using the interference ratio method (Figure S1 and Table S2), we found that the presence of a crossover in one interval decreases the likelihood of crossing over in an adjacent interval (exerts positive interference) in wild-type strains. Similar to our coefficient of coincidence measurements, interference as measured by the interference ratio method in *ecm11*, *ecm11[K5R, K101R]*, *gmc2*, and *zip1-N1* mutant strains appeared weaker than wild type, but not absent, in most interval pairs (Figure S1, Table S2).

The presence of (albeit weakened) crossover interference in *ecm11*, *gmc2*, and *zip1-N1* mutants is consistent with models that propose that SC is not required for interference in budding yeast (Fung *et al.* 2004; Zhang *et al.* 2014a,b).

The fraction of recombination events that resolve to a crossover outcome is the same or diminished in ecm11 mutant meiotic cells relative to wild type

One explanation for the increased number of interhomolog crossover events in *ecm11*, *gmc2*, and *zip1-N1* mutants is that the number of interhomolog repair intermediates is normal but the absence of central element proteins (or tripartite SC) increases the likelihood that a given interhomolog-engaged repair intermediate is resolved toward a crossover *vs.* a non-crossover outcome. We tested this possibility by measuring the frequency of crossing over associated with meiotic interhomolog recombination events at *ARG4* and *LEU2* in wild-type and *ecm11* strains (Figure 5). Interhomolog recombination events at *ARG4* or *LEU2* were identified by selecting prototrophs among spore products from diploids carrying *arg4* and *leu2* heteroalleles; flanking genetic markers were then used to determine the fraction of interhomolog recombination events associated with a crossover. This experiment revealed that the percentage of recombination events accompanied by a crossover at either locus is similar to or diminished in *ecm11* mutants relative to wild type (51.7 *vs.* 70.4% at *ARG4* and 47.9 *vs.* 47.1% at *LEU2*, respectively; Figure 5). These data suggest that Ecm11's absence does not increase the likelihood that a given interhomolog recombination intermediate is resolved toward a crossover outcome. Alternatively, the presence of SC central region proteins might act to limit the likelihood that initiated recombination events productively engage with the homolog for repair.

A third possibility is that the presence of SC central region proteins may directly or indirectly downregulate the number of recombination events that are initiated during meiotic prophase. This possibility is supported by the recent demonstration of elevated recombination initiation (Spo11-mediated DNA double strand breaks) in *zip1*, *zip3*, *zip4*, and *spo16* mutants, which are missing proteins with both procrossover and pro-SC assembly roles (Thacker *et al.* 2014). If the same feedback mechanism that leads to increased Spo11-mediated recombination initiation in *zip1*, *zip3*, *zip4*, and *spo16* mutants is responsible for the elevated number of MutSγ-mediated crossovers we observe in *ecm11*, *gmc2*, and *zip1-N1* mutants, this would suggest the interesting possibility that the feedback mechanism itself is coupled to a deficit in tripartite SC, rather than to a deficit in SIC protein-mediated crossover activity.

ecm11 and gmc2, but not zip1-N1 mutants, display delayed progression through late prophase

While, in principle, the SC may directly prevent recombination initiation or influence how recombination events are processed, we note two alternative models (which are not mutually exclusive) in which the presence of SC central element proteins prevent elevated crossing over indirectly. First, an increase in crossovers might not be the result of absent tripartite SC *per se* but instead due to a diminished level of a particular SC-associated protein, which has a dual role in SC assembly and crossover control. One example candidate for such a factor is SUMOylated Ecm11, as Ecm11 SUMOylation is required for SC assembly and is impaired in both *gmc2* and *zip1-N1* mutants (Humphryes *et al.* 2013; Figure 4).

Second, the excess MutSγ crossovers observed in *ecm11*, *gmc2*, and *zip1-N1* mutants may derive from additional recombination events that are initiated and processed specifically

Genotype	Sporulation efficiency (n)	Frequency of sporulated products that are Arg^+ $X10^{-3}$ (SD)	% of Arg^+ (n) with an associated crossover	% Crossing over on chr.III among Arg^+ (n)		Frequency of sporulated products that are Leu^+ $X10^{-4}$ (SD)	% of Leu^+ (n) with an associated crossover	% Crossing over on chr.VIII among Leu^+ (n)	
			SPO13-THR1	*HIS4-CEN3*	*CEN3-MAT*		*HIS4-CEN3*	*CEN8-SPO13*	*SPO13-THR1*
ZIP1 (K794)	54% (2207)	17.8 (2.2)	**70.4** (961)	**24** (233)	**17** (168)	24.8 (8.0)	**47.1** (718)	**18** (127)	**7** (50)
ecm11Δ (K829)	48% (1925)	42.2 (2.6)	**51.7** (917)	**26** (237)	**32** (296)	24.4 (6.2)	**47.9** (797)	**27** (213)	**21** (164)
zip1Δ (K826)	7% (2074)	92.4 (16.3)	n.d.	n.d.		43.4 (7.6)	n.d.	n.d.	

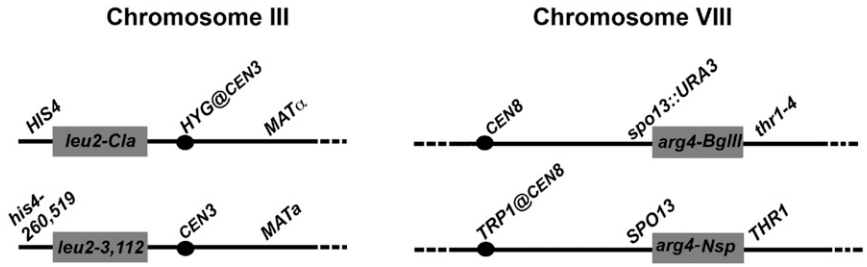

Figure 5 The fraction of recombination events associated with a crossover does not increase in *ecm11* meiotic cells. A total of three to five independent cultures of wild-type, *ecm11*, and *zip1* strains transheterozygous for the *arg4-Nsp*, *arg4-BglII*, and the *leu2-Cla1*, *leu2-3,112* heteroalleles were assessed for prototroph formation at *ARG4* and *LEU2*. The values given in the third and seventh columns are the average measurement of the fraction of cells that are Arg^+ or Leu^+ after 3 days of liquid sporulation. For each strain, the fraction of Arg^+ and Leu^+ cells in vegetative cultures at the time of transfer to sporulation medium was also measured; the median of independent replicates for each strain were as follows: (for Arg^+) *WT*, 3.7×10^{-5}; *ecm11*, 8.1×10^{-5}; and *zip1*, 8×10^{-5} and (for Leu^+) *WT*, 1.9×10^{-6}; *ecm11*, 1.9×10^{-6}; and *zip1*, 4.9×10^{-6}. The values given in the sporulation efficiency column are the percentage of sporulated products containing two, three, or four spores. In columns 4 and 8 is the percentage of all selected heteroallelic recombination events associated with a crossover outcome (crossovers were measured in haploid recombinants, using flanking markers indicated in the cartoon below). Crossover frequency was also assessed in intervals that are unassociated with the selected heteroallelic recombination event (columns 5, 6, 9, and 10); for *ARG4* heteroallelic recombination, crossover frequency was assessed in two intervals on chromosome III; and for *LEU2* heteroallelic recombination, crossover frequency was assessed in two intervals on chromosome VIII.

during a protracted prophase; such a delay in prophase progression could be caused by a checkpoint triggered by the absence of tripartite SC or SC central element proteins. Indeed, an *ndt80* mutation-induced prophase arrest was found to rescue deficiencies in spore viability, synapsis, and interhomolog recombination for some *spo11* hypomorphic strains (Rockmill *et al.* 2013), an *ndt80* mutation-induced prophase arrest was separately found to be associated with elevated recombination initiation in otherwise wild-type cells (Allers and Lichten 2001; Thacker *et al.* 2014), and elevated interhomolog recombination has been observed in mutants such as *zip3*, *zip1*, and *msh5*, which exhibit a dual deficit in SC assembly and SC-associated crossing over and have a protracted prophase (Thacker *et al.* 2014). It is noteworthy that in the case of mutants with a dual deficit in SC assembly and SC-associated crossing over, the extent of elevated interhomolog recombination or recombination initiation could not be fully explained by a protracted prophase alone (Rockmill *et al.* 2013; Thacker *et al.* 2014), suggesting that either a procrossover or an SC assembly activity (or both) can directly modulate interhomolog recombination. Nevertheless, the possibility exists that increased duration in prophase alone, due to a checkpoint response triggered by an SC deficiency, can potentially allow for the accumulation of interhomolog recombination events (including MutSγ-mediated crossovers) in crossover proficient, SC-deficient mutants such as *ecm11*, *gmc2*, and *zip1-N1*.

To explore whether an increase in MutSγ crossing over in SC central element-deficient mutants might be due to a prolonged prophase, we examined the morphology of DAPI-stained, surface-spread nuclei and associated spindle structures from wild-type, *ecm11*, *ecm11[K5R, K101R]*, and *zip1-N1* cells in liquid sporulation media at multiple time points (Figure S2A). We also used DAPI staining on whole-mount cells cultured on solid sporulation media to measure the frequency of meiocytes, at multiple time points, that had undergone a meiotic division (Figure S2B). Consistent with a prior study, we found that *ecm11* mutants exhibit a delay in exiting meiotic prophase (Figure S2 and Humphryes *et al.* 2013). In our liquid sporulation time course experiment, by 28 hr, ~50% of surface-spread nuclei from wild-type meiocytes had progressed beyond the pachytene stage and a substantial fraction were undergoing meiotic divisions. In

contrast, DAPI morphology and spindle structures indicated that nearly all *ecm11* and *ecm11[K5R, K101R]* mutant meiocytes were at pachytene at this 28-hr time point (Figure S2A). Similarly, our analysis of meiocytes cultured on solid sporulation media revealed a lag in the accumulation of multinucleate cells in *ecm11* null, *ecm11[K5R, K101R]*, and *gmc2* null mutants relative to wild type (Figure S2B).

However, both of our meiotic progression analyses revealed that *zip1-N1* mutant meiocytes progress through pachytene and enter meiotic divisions with similar kinetics as wild-type meiocytes (Figure S2, A and B), making a meiotic prophase checkpoint less likely to account for *zip1-N1*'s excess crossover recombination phenotype.

Our analysis suggests that the excess MutSγ crossovers observed in *ecm11*, *ecm11[K5R, K101R]*, *gmc2*, and *zip1-N1* mutants accumulate independent of a protracted prophase. These data may also reveal insight into how recombination intermediates that form during a protracted prophase are processed in budding yeast. It is interesting to note that while *ecm11*, *ecm11[K5R, K101R]*, *gmc2*, and *zip1-N1* mutants share the same excess crossover phenotype, *ecm11*, *ecm11[K5R, K101R]*, and *gmc2* mutants exhibit a prolonged prophase as well as a set of excess noncrossover interhomolog recombination events that are not present in *zip1-N1* mutants (Table S1). These *ecm11*- and *gmc2*-specific phenotypes suggest that interhomolog recombination intermediates formed during the protracted prophase of *ecm11* and *gmc2* mutants may largely be resolved with a noncrossover outcome.

Conclusions

Our data first and foremost demonstrate that tripartite SC is dispensable for the procrossover activities of Zip1, Zip2, Zip3, Zip4, Spo16, Msh4, and Msh5 proteins. The *ecm11*, *gmc2*, and *zip1-N1* mutant phenotypes reveal that two classes of SC proteins exist in budding yeast, one that has both pro-SC and procrossover functions, and a second one that is specifically dedicated to SC assembly. This discovery suggests that the procrossover function of Zip2, Zip3, Zip4, Spo16, and Zip1 is not based on a role in assembling tripartite SC, but is an independent activity altogether. What are the specific roles of these SC-associated proteins in crossover recombination? Our recent observation that an ancestrally related version of the transverse filament protein, *Kluyveromyces lactis* Zip1, can rescue crossover recombination in a Zip3-, Zip4-, Spo16-, and Mlh3-dependent but Msh4-independent manner suggests that SC transverse filament proteins have a specialized role in processing recombination intermediates, perhaps even in a manner that parallels or overlaps the activities of MutSγ complexes (Voelkel-Meiman *et al.* 2015). It will be of particular interest to understand the molecular basis for how budding yeast SC transverse filament proteins promote the maturation of crossover-designated recombination intermediates and to learn whether the functional relationship between transverse filament proteins and recombination mechanics is conserved in other organisms.

Our analysis of *ecm11*, *gmc2*, and *zip1-N1* mutants also demonstrates that MutSγ-mediated interhomolog crossovers are limited, either directly or indirectly, by the presence of SC central element proteins. These data are not the first to suggest a link between an antirecombination function and the budding yeast SC (Allers and Lichten 2001; Rockmill *et al.* 2013; Thacker *et al.* 2014). However, prior studies that correlated budding yeast SC with a constraint on interhomolog recombination involved mutants missing proteins required for both crossing over and SC assembly, leaving open the question of whether the procrossover activity or the SC is key to the mechanism that limits recombination. The data we present here hone in on the SC itself, independent of any procrossover activity, as the relevant molecular entity that is linked to limiting MutSγ-mediated interhomolog crossing over. Taken together with recent studies that have observed excess crossing over caused by alterations in the abundance or structure of SC components in *C. elegans* and rice (Libuda *et al.* 2013; Wang *et al.* 2015), our data add weight to the idea that a conserved role of the SC structure is to limit interhomolog recombination.

Acknowledgments

We thank Scott Holmes for comments on the manuscript. A National Institutes of Health grant to A.J.M., R15-GM104827, supported this work.

Literature Cited

Allers, T., and M. Lichten, 2001 Differential timing and control of noncrossover and crossover recombination during meiosis. Cell 106: 47–57.

Borner, G. V., N. Kleckner, and N. Hunter, 2004 Crossover/noncrossover differentiation, synaptonemal complex formation and regulatory surveillance at the leptotene/zygotene transition of meiosis. Cell 1127: 29–45.

Chua, P. R., and G. S. Roeder, 1998 Zip2, a meiosis-specific protein required for the initiation of chromosome synapsis. Cell 93: 349–359.

De Muyt, A., L. Jessop, E. Kolar, A. Sourirajan, J. Chen *et al.*, 2012 BLM helicase ortholog Sgs1 is a central regulator of meiotic recombination intermediate metabolism. Mol. Cell 46: 43–53.

Dong, H., and G. S. Roeder, 2000 Organization of the yeast Zip1 protein within the central region of the synaptonemal complex. J. Cell Biol. 148: 417–426.

Fung, J. C., B. Rockmill, M. Odell, and G. S. Roeder, 2004 Imposition of crossover interference through the nonrandom distribution of synapsis initiation complexes. Cell 116: 795–802.

Game, J. C., 1992 Pulsed-field gel analysis of the pattern of DNA double-strand breaks in the *Saccharomyces* genome during meiosis. Dev. Genet. 13: 485–497.

Game, J. C., K. C. Sitney, V. E. Cook, and R. K. Mortimer, 1989 Use of a ring chromosome and pulsed-field gels to study interhomolog recombination, double-strand DNA breaks and sister-chromatid exchange in yeast. Genetics 123: 695–713.

Hamer, G., K. Gell, A. Kouznetsova, I. Novak, R. Benavente *et al.*, 2006 Characterization of a novel meiosis-specific protein within the central element of the synaptonemal complex. J. Cell Sci. 119: 4025–4032.

Hooker, G. W., and G. S. Roeder, 2006 A role for SUMO in meiotic chromosome synapsis. Curr. Biol. 16: 1238–1243.

Humphryes, N., W. K. Leung, B. Argunhan, Y. Terentyev, M. Dvorackova *et al.*, 2013 The Ecm11-Gmc2 complex promotes synaptonemal complex formation through assembly of transverse filaments in budding yeast. PLoS Genet. 9: e1003194.

Hunter, N., and N. Kleckner, 2001 The single-end invasion: an asymmetric intermediate at the double-strand break to double-Holliday junction transition of meiotic recombination. Cell 106: 59–70.

Jessop, L., B. Rockmill, G. S. Roeder, and M. Lichten, 2006 Meiotic chromosome synapsis-promoting proteins antagonize the anti-crossover activity of Sgs1. PLoS Genet. 2: e155.

Kee, K., and S. Keeney, 2002 Functional interactions between *SPO11* and *REC102* during initiation of meiotic recombination in *Saccharomyces cerevisiae*. Genetics 160: 111–122.

Kolas, N. K., and P. E. Cohen, 2004 Novel and diverse functions of the DNA mismatch repair family in mammalian meiosis and recombination. Cytogenet. Genome Res. 107: 216–231.

Libuda, D. E., S. Uzawa, B. J. Meyer, and A. M. Villeneuve, 2013 Meiotic chromosome structures constrain and respond to designation of crossover sites. Nature 502: 703–706.

Malkova, A., J. Swanson, M. German, J. H. McCusker, E. A. Housworth *et al.*, 2004 Gene conversion and crossing over along the 405-kb left arm of *Saccharomyces cerevisiae* chromosome VII. Genetics 168: 49–63.

Nishant, K. T., C. Chen, M. Shinohara, A. Shinohara, and E. Alani, 2010 Genetic analysis of baker's yeast Msh4-Msh5 reveals a threshold crossover level for meiotic viability. PLoS Genet. 6: e1001083.

Novak, J. E., P. Ross-Macdonald, and G. S. Roeder, 2001 The budding yeast Msh4 protein functions in chromosome synapsis and the regulation of crossover distribution. Genetics 158: 1013–1025.

Page, S. L., and R. S. Hawley, 2004 The genetics and molecular biology of the synaptonemal complex. Annu. Rev. Cell Dev. Biol. 20: 525–558.

Papazian, H. P., 1952 The analysis of tetrad data. Genetics 37: 175–188.

Rockmill, B., 2009 Chromosome spreading and immunofluorescence methods in Saccharomyes cerevisiae. Methods Mol. Biol. 558: 3–13.

Rockmill, B., and G. S. Roeder, 1998 Telomere-mediated chromosome pairing during meiosis in budding yeast. Genes Dev. 12: 2574–2586.

Rockmill, B., P. Lefrancois, K. Voelkel-Meiman, A. Oke, G. S. Roeder *et al.*, 2013 High throughput sequencing reveals alterations in the recombination signatures with diminishing Spo11 activity. PLoS Genet. 9: e1003932.

Shinohara, M., S. D. Oh, N. Hunter, and A. Shinohara, 2008 Crossover assurance and crossover interference are distinctly regulated by the ZMM proteins during yeast meiosis. Nat. Genet. 40: 299–309.

Storlazzi, A., L. Xu, A. Schwacha, and N. Kleckner, 1996 Synaptonemal complex (SC) component Zip1 plays a role in meiotic recombination independent of SC polymerization along the chromosomes. Proc. Natl. Acad. Sci. USA 93: 9043–9048.

Sym, M., and G. S. Roeder, 1994 Crossover interference is abolished in the absence of a synaptonemal complex protein. Cell 79: 283–292.

Sym, M., J. Engebrecht, and G. S. Roeder, 1993 Zip1 is a synaptonemal complex protein required for meiotic chromosome synapsis. Cell 72: 365–378.

Thacker, D., N. Mohibullah, X. Zhu, and S. Keeney, 2014 Homologue engagement controls meiotic DNA break number and distribution. Nature 510: 241–246.

Tsubouchi, T., H. Zhao, and G. S. Roeder, 2006 The meiosis-specific Zip4 protein regulates crossover distribution by promoting synaptonemal complex formation together with Zip2. Dev. Cell 10: 809–819.

Tung, K.-S., and G. S. Roeder, 1998 Meiotic chromosome morphology and behavior in *zip1* mutants of *Saccharomyces cerevisiae*. Genetics 149: 817–832.

Voelkel-Meiman, K., L. F. Taylor, P. Mukherjee, N. Humphryes, H. Tsubouchi *et al.*, 2013 SUMO localizes to the central element of synaptonemal complex and is required for the full synapsis of meiotic chromosomes in budding yeast. PLoS Genet. 9: e1003837.

Voelkel-Meiman, K., C. Johnston, Y. Thappeta, V. V. Subramanian, A. Hochwagen *et al.*, 2015 Separable Crossover-Promoting and Crossover-Constraining Aspects of Zip1 Activity during Budding Yeast Meiosis. PLoS Genet. 11: e1005335.

Wang, K., C. Wang, Q. Liu, W. Liu, and Y. Fu, 2015 Increasing the genetic recombination frequency by partial loss of function of the synaptonemal complex in rice. Mol. Plant 8: 1295–1298.

Xu, L., M. Ajimura, R. Padmore, C. Klein, and N. Kleckner, 1995 *NDT80*, a meiosis-specific gene required for exit from pachytene in *Saccharomyces cerevisiae*. Mol. Cell. Biol. 15: 6572–6581.

Zakharyevich, K., S. Tang, Y. Ma, and N. Hunter, 2012 Delineation of joint molecule resolution pathways in meiosis identifies a crossover-specific resolvase. Cell 149: 334–347.

Zhang, L., E. Espagne, A. de Muyt, D. Zickler, and N. E. Kleckner, 2014a Interference-mediated synaptonemal complex formation with embedded crossover designation. Proc. Natl. Acad. Sci. USA 111: E5059–E5068.

Zhang, L., S. Wang, S. Yin, S. Hong, K. P. Kim *et al.*, 2014b Topoisomerase II mediates meiotic crossover interference. Nature 511: 551–556.

Communicating editor: N. Hunter

GENETICS

Supporting Information
www.genetics.org/lookup/suppl/doi:10.1534/genetics.115.182923/-/DC1

Synaptonemal Complex Proteins of Budding Yeast Define Reciprocal Roles in MutSγ-Mediated Crossover Formation

Karen Voelkel-Meiman, Shun-Yun Cheng, Savannah J. Morehouse, and Amy J. MacQueen

DOI: 10.1534/genetics.115.182923

MacQueen_Figure S1

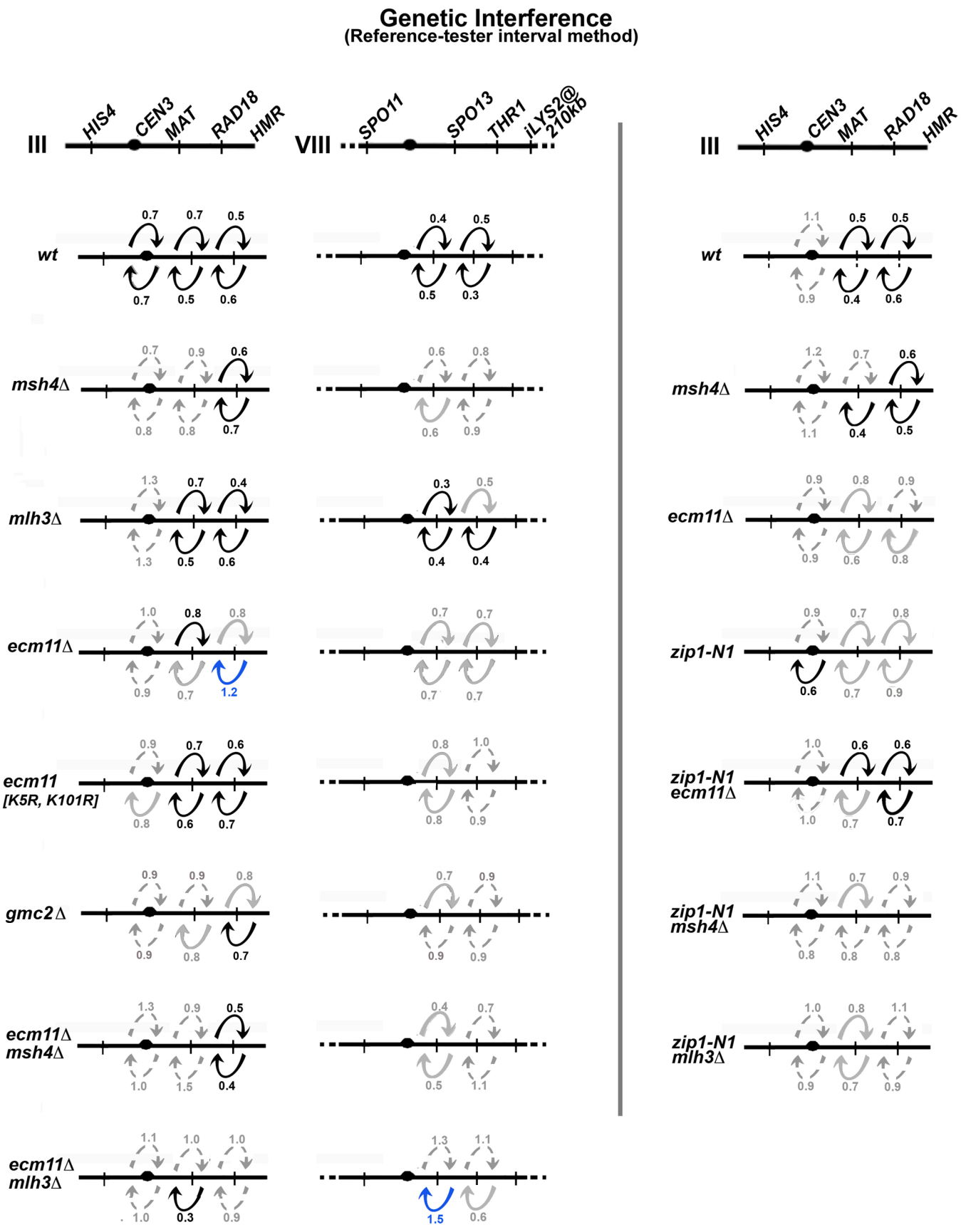

MacQueen_Figure S2

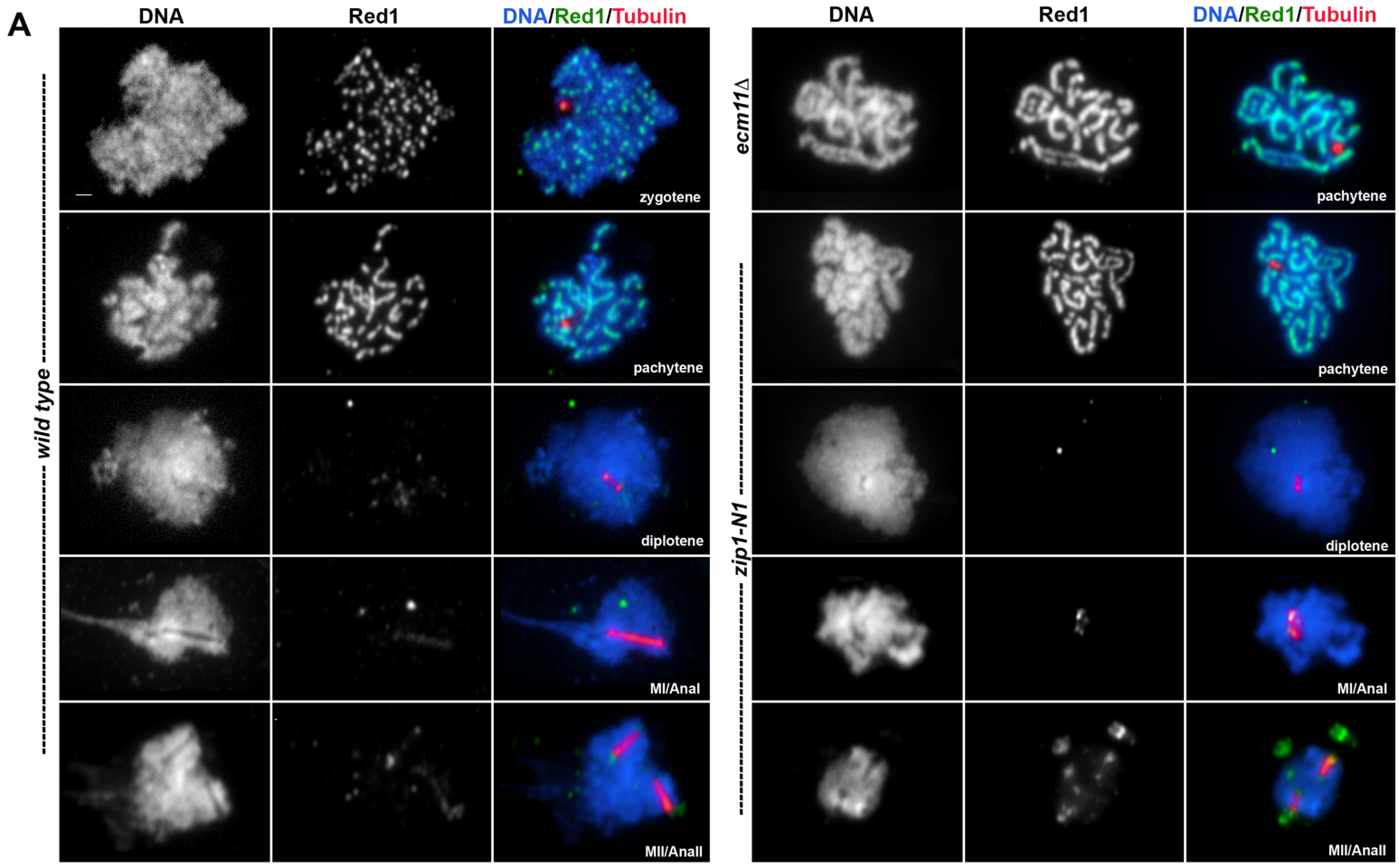

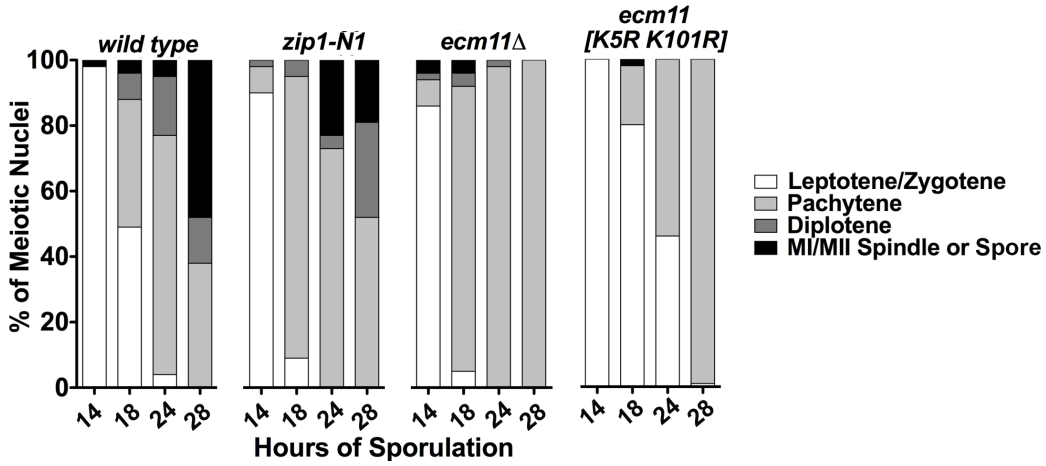

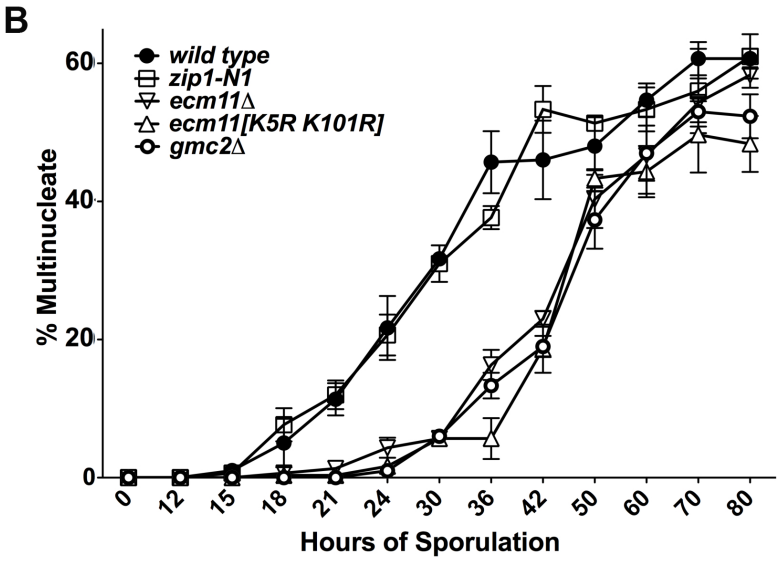

Table S1. Non-mendelian segregation events

% of events that are 3:1/1:3			CHROMOSOME III					CHROMOSOME VIII					
Genotype	(strain #)	4 spore viable tetrads	*HIS4*	*hphMX@ CEN3*	*MAT*	*ADE2 @ RAD18*	*natMX@ HMR*	*TRP1MX @ SPO11*	*spo13:: URA3*	*THR1*	*LYS2 @ chrm VIII* (210kb)	**Sum 3:1/1:3 % total**	**Mutant/WT fold increase**
WT	(K842)	682	1.0	0.0	0.1	1.0	0.3	1.2	0.3	2.9	0.0	**6.8**	**1.0**
msh4Δ	(K852)	478	1.5	0.2	0.4	2.3	0.2	3.8	0.8	4.4	0.2	**13.8**	**2.0**
mlh3Δ	(K854)	527	0.2	0.2	0.9	1.1	0.4	2.1	0.2	2.1	0.4	**7.6**	**1.1**
ecm11Δ	(K857)	885	5.2	1.1	4.9	8.6	3.5	5.8	2.9	13.0	4.7	**49.7**	**7.3**
ecm11 [K5R,K101R]	(K846)	644	2.5	1.2	2.6	6.5	2.0	6.7	3.1	14.8	2.6	**42.0**	**6.2**
gmc2Δ	*(K906)*	485	3.5	2.3	3.3	7.6	2.3	5.4	1.9	10.7	3.9	**40.9**	**6.0**
ecm11Δ msh4Δ	(K882)	421	2.6	1.0	2.1	4.5	1.0	5.0	1.4	8.6	1.7	**27.9**	**4.1**
ecm11Δ mlh3Δ	(K888)	506	7.9	4.0	11.5	15.4	10.7	10.3	8.9	18.4	12.5	**99.6**	**14.6**
WT	(YT131)	503	1.0	0.0	1.0	1.5	0.2	3.6	0.0	n.a.	n.a.	**7.3**	**1.0**
msh4Δ	(AM3313)	629	2.4	0.2	1.6	2.2	0.6	4.6	0.5	n.a.	n.a.	**12.1**	**1.7**
ecm11Δ	(AM3378)	400	4.3	1.5	5.3	8.3	2.0	7.0	3.8	n.a.	n.a.	**32.2**	**4.4**
zip1-N1	(SYC123)	611	4.4	0.7	1.1	2.6	0.8	5.1	0.8	n.a.	n.a.	**15.5**	**2.5**
zip1-N1 ecm11Δ	(SYC142)	795	3.5	0.6	1.4	4.0	1.1	5.0	0.5	n.a.	n.a.	**16.1**	**2.8**
zip1-N1 msh4Δ	(SYC151)	616	2.6	0.3	1.5	1.8	0.8	6.0	0.3	n.a.	n.a.	**13.3**	**2.7**
zip1-N1 mlh3Δ	(SYC133)	500	4.2	1.2	1.2	1.8	0.8	4.6	0.8	n.a.	n.a.	**14.6**	**2.7**
% of events that are 4:0/0:4												**Sum 4:0/0:4 % total**	
WT	(K842)	682	0.0	0.0	0.0	0.0	0.0	0.0	0.0	0.0	0.0	**0.0**	
msh4Δ	(K852)	478	0.0	0.0	0.0	0.0	0.0	0.2	0.0	0.0	0.0	**0.2**	
mlh3Δ	(K854)	527	0.0	0.0	0.0	0.0	0.0	0.0	0.0	0.0	0.2	**0.2**	
ecm11Δ	(K857)	885	0.0	0.0	0.1	0.2	0.1	0.2	0.0	0.3	0.7	**1.6**	
ecm11[K5R,K101R]	(K846)	644	0.2	0.0	0.2	0.3	0.2	0.0	0.0	0.5	0.0	**1.4**	
gmc2Δ	*(K906)*	485	0.0	0.0	0.0	0.2	0.0	0.0	0.0	0.4	0.2	**0.8**	
ecm11Δ msh4Δ	(K882)	421	0.0	0.0	0.2	0.0	0.0	0.0	0.0	1.2	0.2	**1.6**	
ecm11Δ mlh3Δ	(K888)	506	0.4	0.2	0.2	2.0	1.2	0.4	0.8	0.8	0.2	**6.2**	
WT	(YT131)	503	0.0	0.0	0.0	0.0	0.0	0.0	0.0	n.a.	n.a.	**0.0**	
msh4Δ	(AM3313)	629	0.0	0.0	0.0	0.2	0.2	0.2	0.0	n.a.	n.a.	**0.6**	
ecm11Δ	(AM3378)	400	0.0	0.0	0.0	0.0	0.0	0.0	0.0	n.a.	n.a.	**0.0**	
zip1-N1	(SYC123)	611	0.5	0.0	0.0	0.0	0.2	0.2	0.0	n.a.	n.a.	**0.9**	
zip1-N1 ecm11Δ	(SYC142)	795	0.3	0.1	0.0	0.1	0.0	0.1	0.2	n.a.	n.a.	**0.8**	
zip1-N1 msh4Δ	(SYC151)	616	0.2	0.0	0.0	0.0	0.2	0.3	0.0	n.a.	n.a.	**0.7**	
zip1-N1 mlh3Δ	(SYC133)	500	0.2	0.0	0.0	0.0	0.0	0.4	0.0	n.a.	n.a.	**0.6**	

MacQueen Table S2

Genotype		Reference Interval / Test Interval	HIS4-CEN3 / CEN3-MAT	CEN3-MAT / HIS4-CEN	MAT-RAD18 / MAT-RAD18	MAT-RAD18 / CEN3-MAT	MAT-RAD18 / RAD18-HMR	RAD18-HMR / MAT-RAD18	SPO11-SPO13 / SPO13-THR1	SPO11-SPO13 / SPO11-SPO13	SPO13-THR1 / THR1-LYS2	THR1-LYS2 / SPO13-THR1
WT	PD	P:N:T	198:3:143	198:6:217	120:10:293	120:3:132	98:4:153	98:9:287	189:1:56	189:20:351	230:5:330	230:1:64
K842	**cM ± SE**		**23.4 ±1.9**	**30.1 ±2.0**	**41.7 ±2.2**	**29.4 ±2.4**	**34.7 ±2.6**	**43.3 ±2.3**	**12.6 ±1.8**	**42.1 ±2.3**	**31.9 ±1.5**	**11.9 ±1.6**
	TT + NPD	P:N:T	223:1:106	146:0:107	135:4:112	303:1:115	296:2:120	157:5:117	371:0:37	57:1:36	65:0:30	335:0:30
	cM ± SE		**17.0 ±1.6**	**21.2 ±1.6**	**27.2 ±2.7**	**14.4 ±1.3**	**15.8 ±1.5**	**26.3 ±2.7**	**4.5 ±0.7**	**22.3 ±3.9**	**15.8 ±2.4**	**4.1 ±0.7**
	ratio		**0.7**	**0.7**	**0.7**	**0.5**	**0.5**	**0.6**	**0.4**	**0.5**	**0.5**	**0.3**
	χ^2 P		**0.02**	**.007**	**<0.0001**	**<0.0001**	**<0.0001**	**<0.0001**	**<0.0001**	**<0.0001**	**<0.0001**	**<0.0001**
	Sig. SE (cM)		**yes**	**yes**	**yes**	**yes**	**yes**	**yes**	**yes**	**yes**	**yes**	**yes**
msh4Δ	PD	P:N:T	333:1:41	330:1:87	241:6:168	243:0:35	192:0:83	191:5:153	322:0:23	335:3:83	298:2:122	298:0:20
K852	**cM ± SE**		**6.3 ±1.1**	**11.1 ±1.2**	**24.6 ±2.0**	**6.3 ±1.0**	**15.1 ±1.4**	**26.2 ±2.2**	**3.3 ±0.7**	**12.0 ±1.5**	**15.9 ±1.5**	**3.1 ±0.7**
	TT + NPD	P:N:T	91:0:9	43:0:9	34:1:15	181:1::15	159:0:32	84:2:30	101:0:4	26:0:4	22:0:7	125:0:7
	cM ± SE		**4.5 ±1.4**	**8.7 ±2.6**	**21.0 ±6.5**	**5.3 ±1.8**	**8.4 ±1.4**	**18.1 ±4.0**	**1.9 ±0.9**	**6.7 ±3.1**	**12.1 ±4.0**	**2.7 ±1.0**
	ratio		0.7	0.8	0.9	0.8	**0.6**	**0.7**	0.6	0.6	0.8	0.9
	χ^2 P		0.744	0.785	0.353	0.112	**0.001**	**0.003**	0.353	0.612	0.800	0.829
	Sig. SE (cM)		no	no	no	no	**yes**	**yes**	no	**yes**	no	no
mlh3Δ	PD	P:N:T	286:0:79	286:0:127	209:3:198	209:3:68	199:0:81	199:3:201	284:0:33	289:6:178	318:2:154	318:0:34
K854	**cM ± SE**		**10.8 ±1.1**	**15.4 ±1.1**	**26.3 ±1.7**	**15.4 ±2.2**	**14.5 ±1.4**	**27.2 ±1.7**	**5.2 ±0.9**	**22.6 ±1.8**	**17.5 ±1.4**	**4.8 ±0.8**
	TT + NPD	P:N:T	127:3:25	79:3:25	71:1:34	201:0:35	204:0:30	81:1:29	189:0:7	36:0:7	34:0:7	157:0:7
	cM ± SE		**13.9 ±3.6**	**20.1 ±5.0**	**18.9 ±3.5**	**7.4 ±1.2**	**6.4 ±1.1**	**15.8 ±3.3**	**1.8 ±0.7**	**8.1 ±2.8**	**8.5 ±2.9**	**2.1 ±0.8**
	ratio		1.3	1.3	**0.7**	**0.5**	**0.4**	**0.6**	**0.3**	**0.4**	0.5	**0.4**
	χ^2 P		**0.012**	**0.001**	**0.011**	**0.007**	**<0.0001**	**<0.0001**	**0.006**	**0.013**	0.109	**0.036**
	Sig. SE (cM)		no	no	**yes**	**yes**	**yes**	**yes**	**yes**	**yes**	**yes**	**yes**
ecm11Δ	PD	P:N:T	206:5:237	210:3:177	93:16:256	101:5:176	95:11:160	94:5:210	157:4:127	166:30:286	106:41:308	106:2:105
K857	**cM ± SE**		**29.8 ±1.8**	**25.0 ±1.8**	**48.2 ±3.0**	**36.5 ±2.5**	**42.5 ±3.6**	**38.8 ±2.3**	**26.2 ±2.4**	**48.3 ±3.1**	**60.9 ±3.7**	**27.5 ±2.5**
	TT + NPD	P:N:T	191:8:189	245:2:194	167:13:230	296:8:250	218:14:293	166:24:276	307:4:140	158:9:150	104:12:155	358:6:162
	cM ± SE		**30.5 ±2.4**	**23.4 ±1.5**	**37.6 ±2.6**	**26.9 ±1.8**	**35.9 ±2.2**	**45.1 ±3.0**	**18.1 ±1.7**	**32.1 ±2.9**	**41.9 ±3.7**	**18.8 ±1.7**
	ratio		1.0	0.9	**0.8**	**0.7**	0.8	**1.2**	**0.7**	**0.7**	**0.7**	**0.7**
	χ^2 P		0.305	0.762	**<0.0001**	**<0.0001**	0.193	**0.007**	**0.001**	**<0.0001**	**<0.0001**	**<0.0001**
	Sig. SE (cM)		no	no	**yes**	**yes**	**yes**	**yes**	**yes**	**yes**	**yes**	**yes**
ecm11 [K5R,K101R]	PD	P:N:T	128:5:155	130:5:152	60:22:191	64:8:109	55:10:110	53:21:170	109:0:76	125:24:196	72:28:235	71:0:50
K846	**cM ± SE**		**32.1 ±2.6**	**31.7 ±2.6**	**59.2 ±4.5**	**43.4 ±4.5**	**48.6 ±5.0**	**60.7 ±4.9**	**20.5 ±1.8**	**49.3 ±3.9**	**60.2 ±4.1**	**20.7 ±2.2**
	TT + NPD	P:N:T	161:5:154	162:1:158	112:14:180	225:2:200	191:7:211	119:15:201	273:0:121	96:8:122	52:18:127	262:0:147
	cM ± SE		**28.8 ±2.4**	**25.6 ±1.6**	**43.4 ±3.4**	**24.8 ±1.5**	**30.9 ±2.1**	**43.4 ±3.3**	**15.4 ±1.2**	**37.6 ±3.7**	**59.6 ±5.6**	**18.0 ±1.2**
	ratio		0.9	0.8	**0.7**	**0.6**	**0.6**	**0.7**	**0.8**	**0.8**	1.0	0.9
	χ^2 P		0.351	0.111	**0.0003**	**<0.0001**	**0.0003**	**0.0006**	**0.019**	**0.0001**	0.376	0.286
	Sig. SE (cM)		no	**yes**	**yes**	**yes**	**yes**	**yes**	**yes**	**yes**	no	no
gmc2Δ	PD	P:N:T	98:5:114	95:4:105	48:10:137	53:3:92	24:6:109	23:9:82	82:4:81	85:10:142	51:16:160	50:1:52
K906	**cM ± SE**		**33.2 ±3.3**	**31.6 ±3.2**	**50.5 ±4.4**	**37.2 ±3.7**	**52.2 ±4.7**	**59.7 ±6.9**	**31.4 ±3.8**	**42.6 ±3.8**	**56.4 ±4.7**	**28.2 ±3.6**
	TT + NPD	P:N:T	112:4:130	123:3:132	88:13:141	157:6:152	93:9:201	113:14:196	149:3:97	95:8:103	52:12:117	181:6:126
	cM ± SE		**31.3 ±2.7**	**29.1 ±2.4**	**45.3 ±4.2**	**29.8 ±2.5**	**42.1 ±2.9**	**43.3 ±3.3**	**23.1 ±2.5**	**36.7 ±4.1**	**52.2 ±5.2**	**25.9 ±2.6**
	ratio		0.9	0.9	0.9	**0.8**	**0.8**	**0.7**	**0.7**	0.9	0.9	0.9
	χ^2 P		0.870	0.775	**0.027**	**0.018**	**0.011**	**0.008**	**0.080**	**0.089**	0.350	0.1729
	Sig. SE (cM)		no	no	no	**yes**	**yes**	**yes**	**yes**	no	no	no
ecm11Δ msh4Δ	PD	P:N:T	331:1:22	329:0:47	221:5:141	226:0:17	154:2:81	154:5:129	274:0:32	282:0:52	219:11:103	223:0:22
K882	**cM ± SE**		**4.0 ±1.1**	**6.3 ±0.9**	**23.3 ±2.1**	**3.5 ±0.8**	**19.6 ±2.3**	**27.6 ±2.6**	**5.2 ±0.9**	**7.8 ±1.0**	**25.4 ±3.1**	**4.5 ±1.0**
	TT + NPD	P:N:T	51:0:6	28:0:4	16:0:12	156:1:11	138:2:23	83:0:24	66:0:3	52:0:4	25:0:15	117:0:13
	cM ± SE		**5.3 ±2.0**	**6.3 ±2.9**	**21.4 ±4.7**	**5.1 ±2.0**	**10.7 ±2.9**	**11.2 ±2.0**	**2.2 ±1.2**	**3.6 ±1.7**	**18.8 v3.8**	**5.0 ±1.3**
	ratio		1.3	1.0	0.9	1.5	**0.5**	**0.4**	0.4	0.5	0.7	1.1
	χ^2 P		0.452	1.000	0.758	0.478	**<0.0001**	**<0.0001**	0.167	0.104	0.393	0.852
	Sig. SE (cM)?		no	no	no	no	**yes**	**yes**	**yes**	**yes**	no	no
ecm11Δ mlh3Δ	PD	P:N:T	236:1:78	249:3:79	153:10:124	169:2:578	140:2:68	134:10:109	201:0:35	210:3:115	131:11:156	138:1:31
K888	**cM ± SE**		**13.3 ±1.5**	**14.7 ±1.9**	**32.1 ±3.3**	**39.4 ±0.9**	**19.1 ±2.5**	**33.4 ±3.7**	**7.4 ±1.2**	**20.3 ±2.0**	**37.3 ±3.3**	**10.9 ±2.3**
	TT + NPD	P:N:T	93:1:30	93:1:30	54:4:42	161:0:51	128:2:61	73:4:57	122:1:21	55:4:28	37:5:23	185:0:25
	cM ± SE		**14.5 ±3.0**	**14.5 ±3.0**	**33.0 ±6.0**	**12.0 ±1.5**	**19.1 ±2.7**	**30.2 ±4.6**	**9.4 ±2.5**	**29.9 ±6.8**	**40.8 ±9.7**	**6.0 ±1.1**
	ratio		1.1	1.0	1.0	**0.3**	1.0	0.9	1.3	**1.5**	1.1	0.6
	χ^2 P		0.787	0.992	0.958	**<0.0001**	0.992	0.874	0.439	**0.058**	**0.030**	0.115
	Sig. SE (cM)		no	no	no	**yes**	no	no	no	**yes**	no	**yes**
WT	PD	P:N:T	169:0:86	169:6:159	95:15:227	95:2:90	70:1:116	70:11:210				
YT131	**cM ± SE**		**16.9 ±1.5**	**29.2 ±2.4**	**47.0 ±3.2**	**27.3 ±2.8**	**32.6 ±2.3**	**47.4 ±3.2**				
	TT + NPD	P:N:T	165:3:68	86:2:69	92:1:61	242:1:61	221:4:79	117:5:78				
	cM ± SE		**18.2 ±2.6**	**25.8 ±3.2**	**21.8 ±2.7**	**11.0 ±1.5**	**16.9 ±2.3**	**27.0 ±3.5**				
	ratio		1.1	0.9	**0.5**	**0.4**	**0.5**	**0.6**				
	χ^2 P		0.11	0.66	**<0.0001**	**<0.0001**	**<0.0001**	**<0.0001**				
	Sig. SE (cM)		no	no	**yes**	**yes**	**yes**	**yes**				
msh4Δ	PD	P:N:T	436:2:74	436:2:79	294:10:209	294:3:65	237:5:116	237:11:186				
AM3313	**cM ± SE**		**8.4 ±1.1**	**8.8 ±1.1**	**26.2 ±2.0**	**11.5 ±1.7**	**20.4 ±2.2**	**29.0 ±2.4**				
	TT + NPD	P:N:T	81:1:13	76:1:11	68:2:21	219:0:23	197:2:43	121:11:186				
	cM ± SE		**10.0 ±3.5**	**9.7 ±3.8**	**18.1 ±5.0**	**4.8 ±0.9**	**11.4 ±2.1**	**15.1 ±2.4**				
	ratio		1.2	1.1	0.7	**0.4**	**0.6**	**0.5**				
	χ^2 P		0.69	0.53	**0.01**	**0.005**	**0.0002**	**0.0002**				
	Sig. SE (cM)		no	no	no	**yes**	**yes**	**yes**				
ecm11Δ	PD	P:N:T	65:2:94	65:2:97	27:10:109	30:3:78	29:1:76	27:10:87				
AM3378	**cM ± SE**		**32.9 ±3.1**	**33.2 ±3.0**	**57.9 ±5.7**	**43.2 ±4.6**	**38.7 ±3.3**	**59.3 ±6.7**				
	TT + NPD	P:N:T	94:2:121	93:2:120	74:11:123	129:1:137	99:6:153	74:11:145				
	cM ± SE		**30.7 ±2.4**	**30.1 ±2.5**	**45.4 ±4.5**	**26.8 ±1.8**	**36.6 ±2.9**	**45.9 ±4.1**				
	ratio		0.9	0.9	**0.8**	**0.6**	0.9	0.8				
	χ^2 P		0.822	0.761	**0.002**	**0.0002**	0.075	0.077				
	Sig. SE (cM)		no	no	**yes**	**yes**	no	**yes**				
zip1-N1	PD	P:N:T	80:9:173	0:0:113	28:2:80	0:0:160	48:4:108	60:5:174				
SYC123	**cM ± SE**		**43.3 ±3.3**	**50.0 ±0**	**41.8 ±3.9**	**50.0 ±0**	**41.3 ±3.7**	**42.7 ±2.8**				
	TT + NPD	P:N:T	119:8:185	182:6:187	168:8:109	155:9:208	179:11:180	155:12:179				
	cM ± SE		**37.3 ±2.8**	**29.7 ±2.2**	**27.5 ±3.1**	**35.2 ±2.5**	**33.2 ±2.7**	**36.3 ±3.0**				
	ratio		0.9	**0.6**	**0.7**	**0.7**	**0.8**	**0.9**				
	χ^2 P		0.151	**<0.0001**	**<0.0001**	**<0.0001**	**0.0003**	**<0.0001**				
	Sig. SE (cM)		no	**yes**	**yes**	**yes**	**yes**	**yes**				
zip1-N1 ecm11Δ	PD	P:N:T	105:9:181	102:5:150	63:12:181	65:9:244	76:12:215	72:8:219				
SYC142	**cM ± SE**		**39.8 ±3.0**	**35 ±2.8**	**49.4 ±3.7**	**46.9 ±2.7**	**47.4 ±3.2**	**44.7 ±2.7**				
	TT + NPD	P:N:T	157:9:317	188:7:309	239:9:247	197:9:254	231:8:212	230:13:209				
	cM ± SE		**38.4 ±2.0**	**34.8 ±1.8**	**30.4 ±2.0**	**33.5 ±2.1**	**28.8 ±2.1**	**31.8 ±2.5**				
	ratio		1.0	1.0	**0.6**	**0.7**	**0.6**	**0.7**				
	χ^2 P		0.340	0.659	**<0.0001**	**<0.0001**	**<0.0001**	**<0.0001**				
	Sig. SE (cM)		no	no	**yes**	**yes**	**yes**	**yes**				
zip1-N1 msh4Δ	PD	P:N:T	394:1:88	392:2:96	325:5:161	328:1:82	255:1:150	256:3:136				
SYC151	**cM ± SE**		**9.7 ±1.1**	**11.0 ±1.2**	**19.5 ±1.7**	**10.7 ± 1.2**	**19.2 ±1.4**	**19.5 ±1.7**				
	TT + NPD	P:N:T	102:1:21	89:0:20	82:1:24	168:1:27	142:3:49	151:3:49				
	cM ± SE		**10.9 ±2.9**	**9.2 ±1.9**	**14.0 ±3.4**	**8.4 ±1.9**	**17.3 ±3.0**	**16.5 ±2.9**				
	ratio		1.1	0.8	0.7	0.8	0.9	0.8				
	χ^2 P		0.557	0.761	0.107	0.159	**0.004**	**0.029**				
	Sig. SE (cM)		no	no	**yes**	no	no	no				
zip1-N1 mlh3Δ	PD	P:N:T	179:9:127	177:5:85	127:9:137	127:8:112	126:10:11	126:8:118				
SYC133	**cM ± SE**		**28.7 ±3.0**	**21.5 ±2.8**	**35.0 ±3.3**	**32.4 ±3.5**	**24.2 ±6.2**	**32.9 ±3.4**				
	TT + NPD	P:N:T	95:3:78	135:1:72	119:4:93	147:4:93	127:3:110	120:5:108				
	cM ± SE		**27.3 ±3.3**	**18.8 ±2.1**	**27.1 ±3.1**	**24.0 ±2.8**	**26.7 ±2.6**	**29.6 ±3.1**				
	ratio		1.0	0.9	0.8	0.7	1.1	0.9				
	χ^2 P		0.546	0.350	0.135	0.104	**<0.0001**	0.764				
	Sig. SE (cM)		no	no	**yes**	**yes**	no	no				

MacQueen_Table S3. **Sporulation Efficiency and Spore Viability of Crossover Strains**

Genotype	(Strain)	# Tetrads	% 4 Spore viable	% 3 Spore viable	% 2 Spore viable	% 1 Spore viable	% 0 Spore viable	% Spore viability	% Sporulation efficiency (n)
Figure 1/Table S1									
WT	(K842)	786	92	4	3	0	0	**97**	74 (1134)
msh4Δ	(K852)	1028	42	18	23	15	19	**71**	42 (1005)
mlh3Δ	(K854)	830	65	19	11	3	2	**86**	54 (1000)
ecm11Δ	(K857)	1255	78	15	5	1	1	**92**	41 (1020)
ecm11 [K5R,K101R]	(K846)	801	85	9	5	1	0	**95**	37 (1025)
gmc2Δ	(K906)	633	75	17	8	0	0	**92**	28 (1191)
ecm11Δ msh4Δ	(K882)	1291	33	15	20	15	19	**58**	19 (1017)
ecm11Δ mlh3Δ	(K888)	853	68	18	9	4	1	**87**	36 (1200)
Figure 3/Table S2									
WT	(YT131)	616	86	9	5	1	0	**95**	n.d.
msh4Δ	(AM3313)	1650	39	17	20	12	12	**65**	n.d.
ecm11Δ	(AM3378)	573	74	15	10	1	0	**90**	n.d.
zip1-N1	(SYC123)	744	86	9	3	0	1	**95**	58 (1001)
zip1-N1 ecm11Δ	(SYC142)	1041	81	13	4	1	1	**93**	63 (1247)
zip1-N1 msh4Δ	(SYC151)	1056	59	11	16	3	11	**76**	41 (1243)
zip1-N1 mlh3Δ	(SYC133)	1016	51	27	15	5	2	**80**	59 (1077)

Table S4. Strains used in this study

STRAIN	GENOTYPE
YAM1252	*lys2ΔNhe his4-260,519 leu2-3,112 MAT**α** trp1-289 ura3-1 thr1-4 ade2-1* *lys2ΔNhe his4-260,519 leu2-3,112 MAT**a** trp1-289 ura3-1 thr1-4 ade2-1*
K842 **(Fig. 1)**	*lys2ΔNhe HIS4 leu2-3,112 hphMX4@CEN3 MAT**α** ADE2@RAD18 natMX4@HMR* *lys2ΔNhe his4-260,519 leu2-3,112 CEN3 MAT**a** RAD18 HMR* *trp1-289 ura3-1 TRP1MX4@SPO11 spo13::URA3 THR1 210kb ade2-1* *trp1-289 ura3-1 SPO11 SPO13 thr1-4 LYS2@210kb ade2-1*
K846	K842 homozygous *ecm11[K5R, K101R]*
K852	K842 homozygous *msh4::kanMX4*
K854	K842 homozygous *mlh3::kanMX4*
K857	K842 homozygous *ecm11::LEU2*
K882	K857 homozygous *msh4::kanMX4*
K888	K857 homozygous *mlh3::kanMX4*
K906	K842 homozygous *gmc2::kanMX4*
K479 **(Fig. 2)**	YAM1252 *HIS4 leu2-CUP1 TRP1@CEN3 MAT**α** cup1* *his4-260,519 leu2-3,112 CEN3 MAT**a** CUP1* ***MATα**-bearing chromosome III is circular*
TY261	K479 homozygous *zip4::kanMX4*
TY521	K479 homozygous *zip1::LEU2*
TY522	TY521 homozygous *zip4::kanMX4*
K459	K479 homozygous *msh4::ADE2*
K487	K479 homozygous *zip4::kanMX4 msh4::ADE2*
K491	K479 homozygous *zip1::LEU2 zip4::kanMX4 msh4::ADE2*
K538	K479 homozygous *zip1::URA3 msh4::ADE2*
K551	K479 homozygous *mlh3::hphMX4*
K557	K479 *zip1::LEU2/zip1::URA3* homozygous *mlh3::hphMX4*
K618	K479 homozygous *zip4::kanMX4 mlh3::hphMX4*
K624	K479 homozygous *zip1::LEU2 zip4::kanMX4 mlh3::hphMX4*
K654	K479 homozygous *ecm11::hphMX4*
K660	K654 *zip1::LEU2* *zip1::URA3*
K692	K479 homozygous *msh5::kanMX4*
K720	K654 homozygous *mlh3::kanMX4*
K732	K459 homozygous *ecm11::hphMX4*
K738	K479 homozygous *ecm11[K5R, K101R]*
K754	K654 homozygous *zip4::kanMX4*
K760	K654 homozygous *ndt80::kanMX4*

K802	K654 homozygous *msh5::kanMX4*
K814	K738 homozygous *msh4::kanMX4*
YT131 (Fig. 3)	*HIS4 leu2-3,112 hphMX4@CEN3 MAT**a** ADE2@RAD18 natMX4@HMR trp1-289* *his4-260,519 leu2-3,112 CEN3 MAT**α** RAD18 HMR trp1-289* *ura3-1 SPO11 spo13::URA3 thr1-4 LEU2@ChrmXI152kb 193kb ade2-1* *ura3-1 TRP1MX4@SPO11 SPO13 thr1-4 152kb THR1@193kb ade2-1*
AM3313	YT131 homozygous *msh4::ADE2*
SYC123	YT131 homozygous *zip1-N1 (zip1-N1* encodes Zip1 with residues 21-163 deleted)
AM3378	YT131 homozygous *ecm11::kanMX; ChrmXI 152kb (carries no LEU2 insert)* *ChrmXI 152kb (carries no LEU2 insert)*
SYC133	SYC123 homozygous for *mlh3::kanMX4*
SYC142	SYC123 homozygous for *ecm11::kanMX4*
SYC151	SYC123 homozygous for *msh4::kanMX4*
K231 (Fig. 4)	YAM1252 *ECM11-13MYC::kanMX4 ndt80::LEU2* *ECM11 ndt80::LEU2*
SYC75	K231 homozygous *zip1::URA3*
SYC92	K231 homozygous *zip1-N1 (zip1-N1* encodes Zip1 with residues 21-163 deleted)
AM2712	YAM1252 *ECM11-cMYC::kanMX4 ndt80::LEU2* *ECM11-cMYC::kanMX4 ndt80::LEU2*
SH27	AM2712 homozygous *zip1::URA3*
SYC109	AM2712 homozygous *zip1-N1 (zip1-N1* encodes Zip1 with residues 21-163 deleted)
K794 (Table 5)	YAM1252 *his4-260,519 leu2-3,112 CEN3 MATa TRP1@CEN8 SPO13 arg4-Nsp THR1* *HIS4 leu2-Cla hphMX@CEN3 MATα CEN8 spo13::URA3 arg4-BglII thr1-4*
K826	K794 homozygous *zip1::kanMX*
K829	K794 homozygous *ecm11::kanMX*